4-1-2022

Microglial Inflammation and Cognitive Dysfunction in Comorbid Rat Models of Striatal Ischemic Stroke and Alzheimer's Disease: Effects of Antioxidant Catalase-SKL on Behavioral and Cellular Pathology

Jennifer L. MacKenzie
Schulich School of Medicine & Dentistry

Nadezda Ivanova
Schulich School of Medicine & Dentistry

Hayley J. Nell
Schulich School of Medicine & Dentistry

Courtney R. Giordano
Wayne State University

Stanley R. Terlecky
Hackensack Meridian School of Medicine

See next page for additional authors

NEUROSCIENCE
RESEARCH ARTICLE
J. L. MacKenzie et al. / Neuroscience 487 (2022) 47–65

Microglial Inflammation and Cognitive Dysfunction in Comorbid Rat Models of Striatal Ischemic Stroke and Alzheimer's Disease: Effects of Antioxidant Catalase-SKL on Behavioral and Cellular Pathology

Jennifer L. MacKenzie,[a] Nadezda Ivanova,[a]* Hayley J. Nell,[a] Courtney R. Giordano,[b] Stanley R. Terlecky,[c] Cansu Agca,[d] Yuksel Agca,[d] Paul A. Walton,[a] Shawn N. Whitehead[a] and David F. Cechetto[a]

[a] *Department of Anatomy & Cell Biology, Schulich School of Medicine & Dentistry, Western University, London, ON N6A 5C1, Canada*

[b] *Biobanking and Correlative Sciences Core, Karmanos Cancer Institute/Wayne State University, Detroit, MI 48201, USA*

[c] *Department of Medical Sciences, Hackensack Meridian School of Medicine, Nutley, NJ 07110, USA*

[d] *Department of Veterinary Pathobiology, University of Missouri College of Veterinary Medicine, Columbia, MO 65211, USA*

Abstract—Ischemic stroke often co-occurs with Alzheimer's disease (AD) leading to a worsened clinical outcome. Neuroinflammation is a critical process implicated in AD and ischemic pathology, associated with cognitive decline. We sought to investigate the combined effects of ischemic stroke induced by endothelin-1 injection in two AD rat models, using motor function, memory and microglial inflammation in the basal forebrain and striatum as readouts. In addition, we sought to determine the effectiveness of the antioxidant biologic CAT-SKL in one of the models. The early AD model employed the bilateral intracerebroventricular injections of the toxic β-amyloid peptide $A\beta_{25–35}$, the prodromal AD model used the transgenic Fischer 344 rat overexpressing a pathological mutant human amyloid precursor protein. Motor function was assessed using a cylinder, modified sticky tape and beam-walk tasks; learning and memory were tested in the Morris water maze. Microglial activation was examined using immunohistochemistry. $A\beta_{25–35}$ toxicity and stroke combination greatly increased microglial inflammation in the basal forebrain. Prodromal AD-pathology coupled with ischemia in the transgenic rat resulted in a greater microgliosis in the striatum. Combined transgenic rats showed balance alterations, comorbid $A\beta_{25–35}$ rats showed a transient sensorimotor deficit, and both demonstrated spatial reference memory deficit. CAT-SKL treatment ameliorated memory impairment and basal forebrain microgliosis in $A\beta_{25–35}$ rats with stroke. Our results suggest that neuroinflammation could be one of the early processes underlying the interaction of AD with stroke and contributing to the cognitive impairment, and that therapies such as antioxidant CAT-SKL could be a potential therapeutic strategy.

Key words: comorbidity, memory, neuroinflammation, microglia activation, oxidative stress, catalase.

INTRODUCTION

Alzheimer's disease (AD), the most prevalent type of dementia, and ischemic stroke are very common disorders affecting a large proportion of the world's population. In a large number of cases dementia, including AD, and stroke coincide. The prevalence of stroke comorbidity with dementia among Canadians aged 65 years and older was 1.8%, or 110,000 people, in 2016–2017 (Public Health Agency of Canada, 2020). In the US, the comorbidity of self-reported cognitive decline with stroke in a same age group and similar time period was reported to be 15% (Taylor et al., 2020). Moreover, an interaction between cerebral ischemia and AD pathologies was suggested by epidemiological (Tatemichi et al., 1992; Snowdon, 1997; Esiri et al., 1999; Vermeer et al., 2003; Regan et al., 2006; Cechetto et al., 2008; Thiel et al., 2014; Zhou et al.,

*Corresponding author. Address: Department of Anatomy & Cell Biology, Schulich School of Medicine & Dentistry, Medical Sciences Building, Western University, London, ON N6A 5C1, Canada.
E-mail addresses: nivanov3@uwo.ca (N. Ivanova), giordanoc@karmanos.org (C. R. Giordano), stanley.terlecky@hmhn.org (S. R. Terlecky), agcac@missouri.edu (C. Agca), agcay@missouri.edu (Y. Agca), pwalton@uwo.ca (P. A. Walton), Whitehead@schulich.uwo.ca (S. N. Whitehead), cechetto@uwo.ca (D. F. Cechetto).

Abbreviations: Aβ, amyloid-β; AAF, attending affected forelimb score; AD, Alzheimer's disease; AFU, affected forelimb use score; AP, anterior–posterior; APP, amyloid precursor protein; ANOVA, analysis of variance; CAT-SKL, genetically engineered cell penetrating variant of catalase with a serine-lysine-leucine carboxy terminal consensus sequence; DV, dorsal–ventral; ET-1, endothelin-1; H_2O_2, hydrogen peroxide; ICV, intracerebroventricular; ID, rat identity; MHC, major histocompatibility complex; ML, medial–lateral; MST, modified sticky tape task; MWM, Morris water maze; PCR, polymerase chain reaction; ROI, region of interest; ROS, reactive oxygen species; RP, reverse peptide ($A\beta_{35–25}$); Sal, 0.9% saline; TG, transgenic (Fischer 344 APP21 rat); TZ, target zone used to contain the hidden platform during the learning phase; WT, wildtype (Fischer 344 rat).

https://doi.org/10.1016/j.neuroscience.2022.01.026
0306-4522/

2014)and clinicopathological studies (Snowdon, 1997; Kalaria, 2000; Del Ser et al., 2005; Schneider et al., 2007; Cechetto et al., 2008; Toledo et al., 2013; Attems and Jellinger, 2014)and further supported by findings from research animal models (Whitehead et al., 2005; Whitehead et al., 2005; Whitehead et al., 2007; Whitehead et al., 2010; Amtul et al., 2015; Madigan et al., 2016; Levit et al., 2017). Especially microinfarcts, such as striatal lacunar infarcts, were found to exacerbate cognitive symptoms in individuals with dementia as well as worsen cognitive performance in combined rodent models of AD and cerebral ischemia (Heyman et al., 1998; Esiri et al., 1999; Whitehead et al., 2005; Whitehead et al., 2005; Whitehead et al., 2007; Whitehead et al., 2010; Amtul et al., 2014; Levit et al., 2017). Neuroinflammation and oxidative stress, two processes implicated in the pathogenesis of both AD (Akiyama, 2000; McGeer and McGeer, 2003; Wyss-Coray, 2006; Venkateshappa et al., 2012; Fischer and Maier, 2015; Wojsiat et al., 2018)and brain injury after ischemic stroke (Nogawa et al., 1997; Stoll et al., 1998; Allen and Bayraktutan, 2009; Lakhan et al., 2009; Thiel et al., 2010; Weinstein et al., 2010), were proposed key events underlying the interaction between these disorders from the early disease stage and contributing to the cognitive impairment (Whitehead et al., 2005; Whitehead et al., 2007; Amtul et al., 2015; Amtul, 2015).

Chronic dysregulated neuroinflammation is one of the critical components in the pathogenesis of AD with microglia being one of the key cellular players in the inflammatory cascade (Kinney et al., 2018). Microglial cells respond to brain insults by releasing pro-inflammatory cytotoxic factors and generating reactive oxygen species (ROS) which contributes to the brain tissue damage and neuronal degeneration when this response is not quickly resolved (Heneka et al., 2015). Oxidative stress is evoked by an imbalance in ROS production and the counteracting capabilities of the antioxidant mechanisms of the cell. Accumulation of the amyloid-β (Aβ) protein produced from the amyloid precursor protein (APP), one of the hallmark pathologies in AD, is a potent trigger of ROS and cytokine generation by microglia (Bales et al., 2000; Combs et al., 2001). In turn, ROS activate glial cells to further feed the oxidative environment and potentiate neuroinflammation ultimately propagating the damage. These events appear very early in the prodromal AD stage, far preceding amyloid plaque pathology and highlight a promising treatment avenue (Akiyama, 2000; Nunomura et al., 2001; Wyss-Coray, 2006; Heneka et al., 2015; Kinney et al., 2018). Similar inflammatory and oxidative pathology with profound glial involvement is also implicated in response to ischemia and brain injury (Nogawa et al., 1997; Stoll et al., 1998; Allen and Bayraktutan, 2009; Lakhan et al., 2009; Thiel et al., 2010; Weinstein et al., 2010).

Cholinergic neurons of the basal forebrain region that are essential for normal cognitive functioning were found to be especially susceptible to oxidative damage early in AD (Whitehouse et al., 1982; Collerton, 1989; Auld et al., 2002; Kadowaki et al., 2005; Schliebs, 2005; Geula et al., 2008; Craig et al., 2011). The previous work of our team has demonstrated a cholinergic loss in the basal forebrain which was correlated with increased microglial activation in that region and accompanied by a memory impairment in the $A\beta_{25-35}$ – injected rat model of late-onset sporadic AD (Nell et al., 2015; Nell et al., 2017). These effects of the Aβ toxicity were successfully counteracted by targeted treatment with the antioxidant biologic CAT-SKL (Nell et al., 2017), a genetically engineered cell penetrating variant of the antioxidant enzyme catalase targeted to the cell peroxisomes by virtue of a more efficient peroxisomal targeting signal. Treatment with CAT-SKL has been previously shown to be effective in various *in vitro* models of disease (Wood et al., 2006; Koepke et al., 2007; Young et al., 2008; Undyala et al., 2011; Giordano and Terlecky, 2012; Giordano et al., 2015). Collectively, these findings support the use of the CAT-SKL as a promising therapeutic strategy for disorders with increased oxidative stress and neuroinflammation including AD and cerebral ischemia.

The current study was set to first examine the effect of the comorbidity of striatal ischemic stroke and AD-related brain pathologies on motor function, memory and microglial activation specifically in the basal forebrain and striatum regions. We next examined whether the CAT-SKL antioxidant therapy is able to ameliorate the exacerbated inflammatory pathology and cognitive deficit in the case of comorbidity of cerebral amyloid toxicity with stroke.

We used two previously established rat models of AD in this study. The first model was developed by intracerebroventricular (ICV) injections of neurotoxic $A\beta_{25-35}$ peptide creating a complex neuropathological environment of the early-stages of human late-onset sporadic AD including increased neuroinflammation, cholinergic dysfunction and multi-regional neuronal loss which is accompanied by a memory impairment (Whitehead et al., 2005; Cheng et al., 2006; Whitehead et al., 2007; Zussy et al., 2011; Zussy et al., 2013; Yang et al., 2014; Amtul et al., 2015; Amtul, 2015; Nell et al., 2015; Nell et al., 2017). Since the initial *in vivo* CAT-SKL study was performed employing this AD model (Nell et al., 2017), it was used for the current investigation of the CAT-SKL treatment effects. The second model was a novel APP21 transgenic (TG) Fischer 344 rat overexpressing mutant human APP with Swedish and Indiana mutations implicated in the familial variant of AD (Agca et al., 2008; Silverberg et al., 2015; Au et al., 2016; Levit et al., 2017; Caughlin et al., 2018; Klakotskaia et al., 2018; Weishaupt et al., 2018; Levit et al., 2019; Ivanova et al., 2020; Levit et al., 2020). This rat does not show spontaneous amyloid plaque formation or neuron loss with age, but develops an age-related increase in white matter microglial activation and cognitive changes in the executive and memory domains, thus, recreating the prodromal stage of AD (Baudic et al., 2006; Grober et al., 2008; Prins and Scheltens, 2015; Lee et al., 2016). The small ischemic stroke mimicking conditions seen in humans was induced in both AD models by a unilateral striatal endothelin-1 (ET-1) injection which causes focal cerebral vasoconstriction (Yanagisawa et al., 1988).

The results indicate only a transient forelimb fine motor deficit seen in the $A\beta_{25-35}$-injected rats with ET-1 stroke. The signs of a potential balance disturbance were observed in the combined APP21 TG with stroke rats. Both comorbid rats developed a spatial memory impairment on the Morris water maze (MWM) probe trial where an increased latency to first entry to the target zone was observed. The behavioral methods and representative results of the APP21 TG model were originally presented by supplementary video in (Au et al., 2016) and the results are comprehensively discussed in the current manuscript. Microglial activation was significantly increased in the basal forebrain region of the $A\beta_{25-35}$ – injected rats combined with striatal stroke and, on the contrary, only in the striatal infarct area of the ET-1 – injected APP21 TG Fischer 344 rats. The CAT-SKL treatment demonstrated efficacy in preventing basal forebrain microgliosis and cognitive deficit under conditions of concurrent stroke and cerebral amyloid toxicity in the $A\beta_{25-35}$-injected rats with stroke. These results further support the role of microglial-mediated inflammation in the interaction between cerebral ischemia and AD and their implication in the cognitive impairment beginning as early as the prodromal stage of AD.

EXPERIMENTAL PROCEDURES

Animals and models

All animal handling and procedures were performed in accordance with the Canadian Council on Animal Care guidelines and with approval from the Western University Animal Care Committee (AUP 2008-113; AUP 2014-016). All efforts were made to reduce the numbers of animals used and to minimize their suffering. Male Wistar rats were obtained from Charles River Laboratories (Montreal, QC). Original breeding pairs of male Fischer 344 wildtype (WT) and APP21 TG rats were obtained from Drs. Yuksel Agca and Cansu Agca (University of Missouri, Colombia, MO, USA) (Agca et al., 2008) and subsequently bred in-house. All rats had an *ad libitum* access to food and water and were housed at 22–24 °C under 12 h:12 h light:dark cycle. Rats were kept separate until six months of age (the start of the study), then individually for 24 h following surgery and after that combined in pairs until the end of the study. The complete study timeline is presented in Fig. 1.

$A\beta_{25-35}$-injected rat model of Alzheimer's disease. $A\beta_{25-35}$ which has been found in the brains of AD patients, but not in control samples (Kubo et al., 2002) and which possess neurotoxic properties of the full-length $A\beta_{42}$ peptide demonstrated both *in vitro* (Yankner et al., 1989; Kowall et al., 1992; Pike et al., 1995; Sigurdsson et al., 1997; Millucci et al., 2009) and *in vivo* (Whitehead et al., 2005; Cheng et al., 2006; Whitehead et al., 2007; Zussy et al., 2011; Zussy et al., 2013; Yang et al., 2014; Amtul et al., 2015; Amtul, 2015; Nell et al., 2015; Nell et al., 2017), was used to model the early stage of late-onset AD-like pathology in this study. The non-toxic reverse peptide (RP) $A\beta_{35-25}$ was used as a control. Both peptide fractions were obtained from Bachem Americas Inc., Torrence CA. Rats received bilateral ICV injections of either $A\beta_{25-35}$ or RP (500 nmol in 25 μL sterile 0.9% saline).

APP21 TG Fischer 344 rat model of Alzheimer's disease. Homozygous APP21 TG rat was developed on a Fischer 344 background using lentiviral gene therapy to deliver a human APP gene containing Swedish and Indiana mutations causally linked to the familial early-onset form of AD (Agca et al., 2008). Homozygosity was confirmed by a PCR analysis of the tissue samples from pups. These rats overexpress a pathogenic human APP in tissues including the brain and produce high levels of $A\beta_{42}$ and $A\beta_{40}$ proteins, however, they do not show cerebral amyloid plaques with age, and thus, are a good model to study prodromal AD pathology (Agca et al., 2008; Rosen, 2012; Silverberg et al., 2015; Levit et al., 2017; Klakotskaia et al., 2018; Weishaupt et al., 2018; Ivanova et al., 2020).

Endothelin-1 (ET-1) model of ischemic stroke. Small striatal stroke was modeled using a potent vasoconstrictor agent ET-1 which induced a transient focal ischemic injury approximately 1 h in duration (Yanagisawa et al., 1988; Whitehead et al., 2005; Whitehead et al., 2007; Amtul et al., 2015; Amtul, 2015). A single injection of Human ET-1 (Sigma-Aldrich Canada Co., Oakville, ON) was delivered unilaterally into the right striatum (60 pmol dissolved in 3 μL sterile 0.9% saline).

Surgical procedures

Surgeries were performed under general anesthesia induced with 3% isoflurane (Baxter Corporation, Mississauga, ON) in oxygen in a Harvard anaesthesia box (Harvard Apparatus, Holliston, MA) connected to a tabletop anesthesia machine (VetEquip Inc., Livermore, CA). Rats were then secured in a stereotaxic surgical apparatus (David Kopf Instruments, Tujunga, CA) with continued gas anesthesia. Animals' body temperature was maintained at 37 °C for the time of surgery via a heating pad.

Injection sites for $A\beta_{25-35}$ or RP were identified using the coordinates of Bregma ±1.4 mm medial–lateral (ML), −0.8 mm anterior-posterior (AP) and −4.0 mm dorsal–ventral (DV) (Paxinos and Watson, 1986). Injections were completed over 20 min per ventricle with an *in situ* period of 3 min after each injection. ET-1 or sterile 0.9% saline (Sal; control) injections were administered at Bregma −3.0 mm ML, +0.5 mm AP and −5.0 mm DV over 5 min and kept *in situ* for 3 min post-injection. All injections were done using a Hamilton® syringe (Hamilton Company, Reno, NV).

Upon completion of stereotaxic injections, rats received 1 mg/kg of the analgesic buprenorphine subcutaneously (0.03 mg/ml, Champion Alstoe Animal Health, Whitby, ON) and 0.03 mL of the antibiotic enrofloxacin intramuscularly (22.7 mg/mL, Baytril®, Bayer HealthCare Animal Health, Mississauga, ON).

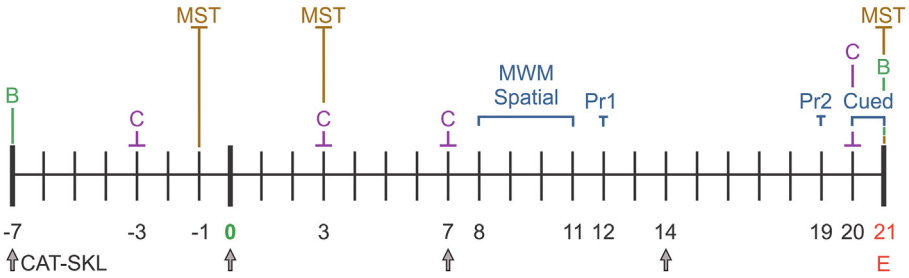

Fig. 1. Timeline for performed behavioral tests and procedures and treatment paradigm. The numbers indicate days of the study relative to the surgery day (0). Surgical operations performed on day 0 as per the assigned treatment group: bilateral intracerebroventricular injection of either $A\beta_{25-35}$ or reverse peptide (RP, $A\beta_{35-25}$); unilateral striatal injection of either endothelin-1 (ET-1) or 0.9% saline. Motor tasks: beam-walk (B), cylinder (C) and modified sticky tape (MST) began with a baseline testing (day -7, -3 and -1, respectively) and were repeated on day 21 for B; days 3 (only for the $A\beta_{25-35}$ – injected rat subset), 7, 20 for C; and days 3, 21 for MST. Morris water maze (MWM) task used to assess cognitive function was completed after all experimental conditions were surgically induced (day 0): spatial learning phase was done through days 8–11, two probe trials (Pr) – on days 12 and 19, cued trials – on days 20 and 21. The arrows indicate time points of the intraperitoneal administration of the antioxidant biologic CAT-SKL, a genetically engineered cell penetrating variant of catalase with a serine-lysine-leucine carboxy terminal consensus sequence, or saline. Rats were euthanized (E) on day 21 post-surgery, brains were perfused and harvested for immunohistochemical analysis.

CAT-SKL treatment

CAT–SKL (United States patent 7601366 and 8663630 and related international patents) was acquired from Drs. Paul A. Walton, Stanley R. Terlecky, and Courtney R. Giordano. The detailed description of synthesis and purification of CAT-SKL is presented elsewhere (Wood et al., 2006; Koepke et al., 2007; Young et al., 2008; Giordano and Terlecky, 2012; Giordano et al., 2015). Wistar rats designated to the CAT-SKL treatment received 1 mg/kg of CAT-SKL intraperitoneally. Rats in the control group were administered a vehicle treatment of an equivalent volume of saline solution via the same route. Both treatments were given once per week for four consecutive weeks starting one week prior to the surgery date as described previously in (Nell et al., 2017) (Fig. 1).

Experimental groups

At the beginning of the study rats were randomly assigned to surgical and treatment groups. Experimental groups and total animal numbers for the first study subset using the $A\beta_{25-35}$ – injected rat AD model were as follows: RP/Sal + Sal n = 6, ET-1 + CAT-SKL n = 8, ET-1 + Sal n = 7, Aβ/ET-1 + CAT-SKL n = 8, Aβ/ET-1 + Sal n = 8. Additionally, Aβ + CAT-SKL (n = 8) and Aβ + Sal (n = 9) groups from a previous study (Nell et al., 2017) were included in the analysis of cognitive testing. Animal groups in the second study subset using the APP21 TG Fischer 344 rat model of AD were WT/Sal n = 8, TG/Sal n = 8, WT/ET-1 n = 9, TG/ET-1 n = 8.

Behavioral testing

All behavioral analysis was done by two separate observers blinded with respect to the rats' identity (ID) and experimental group. The testing days for each behavioral paradigm are depicted on the study timeline (Fig. 1). A detailed description of equipment set up, experimental procedure protocols and analysis can be found in a separate manuscript on the methodology published by our group (Au et al., 2016).

Cylinder task. This task was used for the assessment of forelimb gross motor function during spontaneous rearing in a transparent plexiglass cylinder apparatus (Schallert et al., 2002). It was performed on days -3, 7 and 20 after surgery (day 0) for both experimental subsets and additionally on day 3 post-surgery for the $A\beta_{25-35}$ – injected rat subset (Fig. 1). The task consisted of three 5-min trials a day with a 20-min inter-trial period. Trials with six or more forelimb contacts with the cylinder wall were included in the analysis. The recorded trials were analyzed in iMovie software (Au et al., 2016). The percentage of affected forelimb (i.e. left forelimb) use was calculated for each testing day. The post-surgery results were then divided by a pre-surgery baseline value (day -3) to generate an affected forelimb use (AFU) score for each testing day for each rat individually. An AFU score of 1.0 indicated the equal use of both limbs. An AFU score of less than 1.0 represented a greater use of the unaffected limb and a score of greater than 1.0 signified the opposite. Performance each day was presented as an average of three trials of that day (Au et al., 2016).

Modified sticky tape task (MST). This task was used to assess forelimb fine motor and sensory functions (Sughrue et al., 2006) in the $A\beta_{25-35}$ – injected rat study subset on days -1 (baseline), 3 and 21 after surgery (day 0) with three trials per forelimb per day (Fig. 1). The MST was completed by wrapping a piece of adhesive tape (i.e. tactile stimulus) around one of the rat's forelimbs at a time. A rat was given 45 s to explore the adhesive tape. The affected/unaffected forelimb ratio was then calculated, averaged over trials per day and standardized to an individual baseline level. An attending to affected forelimb (AAF) score was generated and the same scoring system as for the cylinder task was used.

Beam – walk task. This task was implemented to assess the hindlimb motor function with a coordination and balance challenge in the Fischer 344 rat subset (Schallert et al., 2002). Rats underwent the testing on days -7 and 21 in regard to surgery day 0 (Fig. 1). Briefly, rats were required to walk across a 1.9 cm wide wooden beam positioned 40 cm above the ground for three trials in each direction (a total of six trials). The total number of steps per trial and number of hindlimb errors (slips or foot misplacements) per step for each limb were noted from

the recorded videos in iMovie software (Au et al., 2016). Left (i.e. affected) hindlimb errors were standardized to the total number of steps for each testing day. An affected hindlimb error score (AHE score) was generated for each rat individually by subtracting the pre-surgery value from post-surgery value.

Morris water maze (MWM). This task was utilized to evaluate spatial learning and reference memory (Vorhees and Williams, 2006; Vorhees and Williams, 2014). Briefly, in this task rats were required to find an escape platform hidden under the water surface of a pool. Rats were provided with extra-maze cues placed around the pool for navigation. The platform's position in the pool, a quadrant called the target zone (TZ), remained unchanged during the entire learning period. The platform was removed from the tank during the probe trial (Au et al., 2016).

MWM spatial learning phase was completed in 4 days (days 8–11 post-surgery) with four 90 s – trials per day separated by a 20 min inter-trial period (Fig. 1). The probe trials (30 s each) took place on days 12 (Probe 1) and 19 (Probe 2) to assess short-term and long-term spatial reference memory, respectively (Fig. 1). After the end of the day 12 probe the memory was reinforced by placing the platform back to its original position and letting the rats sit on it for 10 s. Cued trials were used as a control for visual impairment (ability to use the extra-maze cues) and lack of motivation to escape the pool and occurred on days 20 and 21 (Fig. 1). The videos were analyzed in ANY-maze® video-tracking software (Stoelting CO, Wood Dale, IL). Distance and latency to reach the platform were used as an indication of spatial and cued learning. Time to first entry to the TZ during the probes was used to assess spatial memory. Swim speed was also recorded (Au et al., 2016).

Euthanasia and tissue processing

On day 21 post surgery, rats were euthanized by a euthanyl overdose (Bimeda-MTC Animal Health Inc., Cambridge, ON). Rats were then transcardially perfused with 0.01 M phosphate-buffered saline solution (PBS, pH 7.35) followed by 4% paraformaldehyde (PFA, pH 7.35). Brains were extracted, post-fixed in 4% PFA for 24 h and then stored in 30% sucrose solution until sliced. Brain tissue was sliced coronally into 35 μm-thick sections from 3.2 to −4.8 mm relative to Bregma on the Cryostar NX50 Cryostat (Thermo Fisher Scientific Inc., Waltham, MA) and stored in cryoprotectant solution at −20 °C until immunohistochemical processing.

Immunohistochemistry

Free-floating brain sections were stained to visualize activated microglia using a primary antibody directed against the major histocompatibility complex II (MHC II) receptor expressed by activated cells (1:1000; OX-6, RT1B purified mouse monoclonal; BD Pharmingen™, Mississauga, ON). Briefly, sections were first washed with 0.1 M PBS and then sequentially incubated with following reagents: 1% H_2O_2 for 10 min at room temperature (RT), 2% horse serum in 0.1 M PBS with Triton-X for 1 h at RT, primary antibody buffer overnight at 4°C, biotinylated horse anti-mouse secondary antibody buffer (1:500; Vector Laboratories Canada Inc., Burlington, ON) for 1 h at RT, 0.05% 3,3′-diaminobenzidine tetrahydrochloride (Sigma Aldrich Canada Co., Oakville, ON) with 1% H_2O_2. After each incubation step, sections were washed in 0.1 M PBS three times for 5 min. Stained sections were mounted on glass slides using 0.3% gelatin, air-dried overnight, then dehydrated by sequential immersion in ethanol solutions of increasing concentration for 5 min each, cleared in 100% Xylene for 10 min and finally cover slipped with Depex media (Electron Microscopy Sciences, Hatfield, PA, USA).

Imaging and quantification

Brain section image acquisition was done on the Nikon Eclipse Ni-E microscope using NIS-Elements Imaging Software Version 4.30.02 (Nikon Instruments Inc., Melville, NY) using x2 and x10 objective lenses. The defined regions of interest (ROI) included the striatum (the infarct area, between Bregma 2.28 mm and −1.44 mm) and the basal forebrain (Bregma 0.96–0.36 mm). Two independent observers blinded to experimental conditions and rats' ID completed the analysis and quantification of inflammation visualized by OX-6 positive microglia using the 64-bit ImageJ software (Version 1.48u4, Wayne Rasband, National Institutes of Health, Bethesda, MD). The volume of OX-6 inflammation in the infarct area in the right striatum was calculated by the formula: $[(\Sigma \text{OX-6 immunostained surface area}) \times (\{n - 1\}\{0.035\}\{0.315\})]$, where n = number of immunostained brain sections, 0.035 mm is the thickness of the brain sections and 0.315 mm is the distance between adjacent sections. OX-6 positive activated microglia cells in the basal forebrain were manually counted in a predefined ROI from four consecutive brain sections generating a single value per animal. These ROI included medial, lateral and paralambdoid septal nuclei, septohippocampal and septohypothalamic nuclei, nucleus of the horizontal and vertical limbs of the diagonal band, lambdoid septal zone.

Statistical analysis

Data analysis was carried out in the GraphPad Prism software (GraphPad Software Inc., La Jolla, CA) version 6.0 and 8.01 (244). The completed statistical tests included one-way, two-way and three-way analysis of variance (ANOVA) followed by a Tukey's or Bonferroni multiple comparisons post hoc test. Data are expressed as the median and interquartile range (25th–75th percentiles), and a minimum of $p \leq 0.05$ was considered statistically significant.

RESULTS

The results of two studies on the comorbidity of AD-like pathology and ischemic stroke are summarized in the

Table 1. Summary of effects of cerebral $A\beta_{25-35}$ toxicity with ischemic stroke comorbidity on motor function, cognitive function and microglial inflammation and their prevention by CAT-SKL antioxidant treatment. Motor function (MF) was assessed using a cylinder task (gross forelimb MF) and modified sticky tape task (fine forelimb MF and sensorium). Cognitive function was assessed in the Morris water maze and parameters included spatial learning, short-term (probe 1; 24 h after last learning day) and long-term (probe 2; 7 days after probe 1) spatial reference memory, and cued learning. Microglial inflammation was examined in the basal forebrain and right striatum (infarct area) using an immunostaining for the activated microglia marker OX-6. Effects were assessed via comparison of parameters at individual testing points between groups: for stroke alone (ET-1 + Sal, ET-1 + CAT-SKL groups) vs control (RP/Sal + Sal) group; for comorbid condition (Aβ/ET-1 + Sal, Aβ/ET-1 + CAT-SKL groups) vs both stroke groups and vs control group. Additionally, effects on all parameters except microglia inflammation, short-term memory and cued learning were compared between different time points within each experimental group. *Statistically significant result ($p \leq 0.05$). Aβ = amyloid β_{25-35} peptide, CAT-SKL = genetically engineered cell penetrating variant of catalase with a serine-lysine-leucine carboxy terminal consensus sequence, ET-1 = endothelin-1, RP = reverse peptide ($A\beta_{35-25}$), Sal = 0.9% saline, Transient deficit – deficit observed at one testing point which then resolved by the end of a test

			Stroke condition alone		Aβ-toxicity and stroke comorbidity	
Treatment			Saline	CAT-SKL	Saline	CAT-SKL
Experimental group			ET-1 + Sal	ET-1 + CAT-SKL	Aβ/ET-1 + Sal	Aβ/ET-1 + CAT-SKL
Motor function (MF)	Gross forelimb		Intact	Transient deficit*	Intact	Intact
	Fine forelimb		Intact	Intact	Transient deficit*	Intact
Cognitive function	Spatial learning		Intact	Intact	Intact	Intact
	Spatial memory	Short-term	Intact	Intact	Intact	Intact
		Long-term	Intact	Intact	Impaired*	Prevented*
	Cued learning		Intact	Intact	Intact	Intact
Microglia activation	Basal forebrain		No change	No change	Increased*	Prevented*
	Right striatum		No change	No change	No change	No change

Table 2. Summary of effects of comorbidity of prodromal AD-like pathology with ischemic stroke in APP21 transgenic Fischer 344 rat on motor function, cognitive function and microglial inflammation. Motor function (MF) was assessed using a cylinder task (gross forelimb MF) and a beam-walk task (gross hindlimb MF, locomotion and gait). Cognitive function was assessed in the Morris water maze and parameters included spatial learning, short-term (probe 1; 24 h after last learning day) and long-term (probe 2; 7 days after probe 1) spatial reference memory, and cued learning. Microglial inflammation was examined in the basal forebrain and right striatum (infarct area) using an immunostaining for the activated microglia marker OX-6. Effects were assessed via comparison of parameters at individual testing points between groups including vs control group (WT/Sal). Additionally, effects on all parameters except microglia inflammation, short-term memory and cued learning were compared between different time points within each experimental group. *Statistically significant result ($p \leq 0.05$). APP = amyloid precursor protein, ET-1 = endothelin-1, Sal = 0.9% saline, TG = APP21 transgenic Fischer 344 rat, WT = wildtype Fischer 344 rat

			Prodromal AD alone	Stroke alone	Prodromal AD and stroke comorbidity
Experimental group			TG/Sal	WT/ET-1	TG/ET-1
Motor function (MF)	Gross forelimb MF		Intact	Intact	Intact
	Gross hindlimb MF		Intact	Intact	Intact
	Balance		Intact	Intact	Impaired*
Cognitive function	Spatial learning		Intact	Intact	Intact
	Spatial memory	Short-term	Intact	Intact	Intact
		Long-term	Intact	Intact	Impaired*
	Cued learning		Intact	Intact	Intact
Microglial activation	Basal forebrain		No change	No change	No change
	Right striatum		No change	No change	Increased*

Table 1 and Table 2 for the $A\beta_{25-35}$ – injected rat model and APP21 TG Fischer 344 rat model, respectively.

Motor function assessment

Comorbid $A\beta_{25-35}$–injected rats with ET-1 ischemic stroke did not develop gross forelimb motor dysfunction and showed only a transient sensorimotor deficit

Groups that received a stroke or sham stroke with an exception of ET-1/CAT-SKL rats did not show a significant impairment of a gross forelimb motor function in the cylinder task, as there was no significant difference in the AFU scores on post-surgery days compared to the baseline level (Fig. 2A). ET-1/CAT-SKL rats were the only group that showed a greater use of the unaffected limb on day 7 post-surgery compared to the baseline ($p = 0.025$) and day 3 ($p = 0.013$).

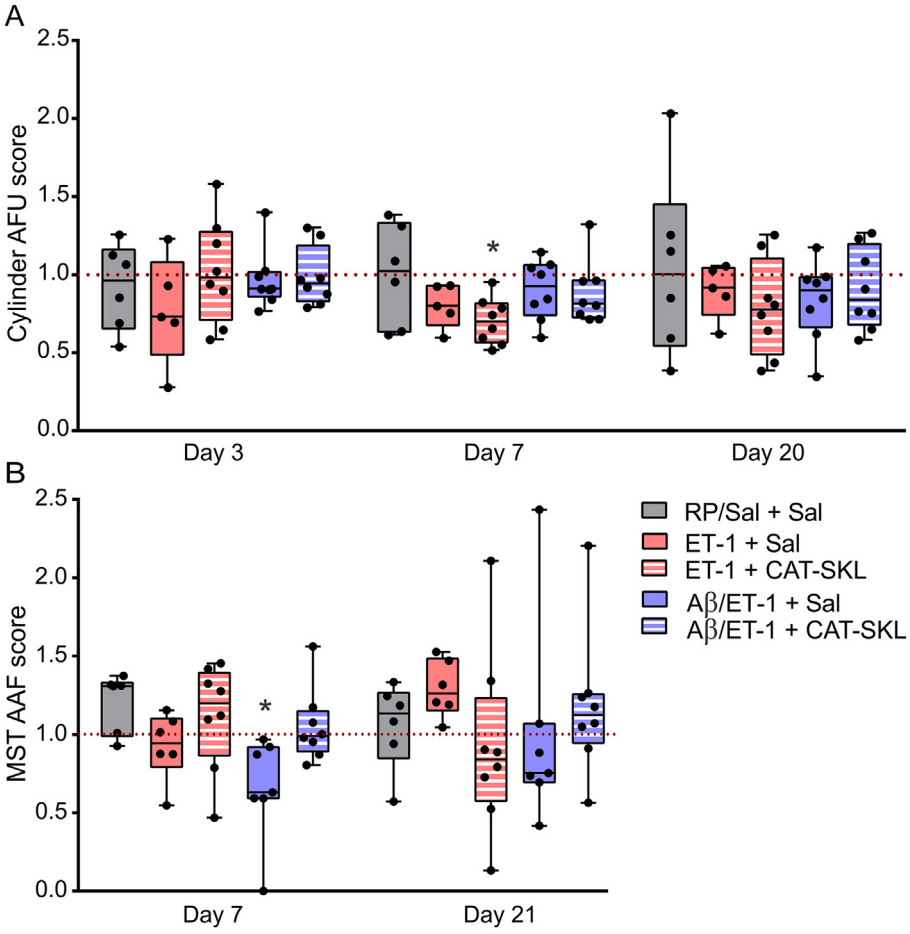

Fig. 2. Forelimb motor function of the comorbid $A\beta_{25-35}$ – injected rats with ET-1 ischemic stroke. **(A)** Affected forelimb use (AFU) scores for the cylinder task and B) attending affected forelimb (AAF) scores for the modified sticky tape (MST) task. The red horizontal dotted line at y = 1.0 indicates an equal use of or attention paid to the forelimbs. A score of less than 1.0 represented a greater use of/attention to the unaffected limb and a score of greater than 1.0 signified the opposite. Each bar represents values standardized to baseline and averaged for three trials per day. Data is presented as median (25th–75th percentiles). Significance is indicated by * in **(A)** between cylinder task days 7 and 3 for ET-1/CAT-SKL group ($p = 0.013$) signifying a greater use of unaffected limb on day 7 compared to day 3 and in **(B)** for Aβ/ET-1 + Sal vs RP/Sal + Sal in day 3 signifying a less attention paid to affected limb with the tape in MST ($p = 0.022$). Repeated measurement two-way ANOVA, Tukey's post hoc test, $p < 0.05$. Aβ = amyloid β_{25-35} peptide, CAT-SKL = genetically engineered cell penetrating variant of catalase with a serine-lysine-leucine carboxy terminal consensus sequence, ET-1 = endothelin-1, RP = reverse peptide ($A\beta_{35-25}$), Sal = 0.9% saline.

However, this effect diminished by the last day of testing, suggesting the improvement of motor function and compensation of the deficit with time (Fig. 2A). Additionally, no differences were observed between the experimental groups within any of the testing days. The presence of AD-like pathology did not lead to a worse motor function in the comorbid $A\beta_{25-35}$ – injected rats (Aβ/ET-1 groups) with or without CAT-SKL when compared to the stroke condition alone (Fig. 2A).

The fine forelimb motor function and tactile senses were unchanged following a stroke in all surgical groups as evidenced by the absence of significant differences in the AAF scores (time spent attending to affected forelimb) between the testing days in the MST task (Fig. 2B). However, when the group performance within each day was analyzed, comorbid Aβ/ET-1 + Sal rats paid significantly less attention to the affected limb with the tape on day 3 post-surgery compared to control RP/Sal + Sal rats (Fig. 2B, $p = 0.022$). This effect was considered transient since the scores were no longer different between the groups on day 21 post-stroke.

Comorbid APP21 TG Fischer 344 rats with ET-1 ischemic stroke showed no forelimb or hindlimb gross motor dysfunction

As shown in Fig. 3A, APP21 TG rats recovering from the ischemic stroke (TG/ET-1 group) did not experience significant forelimb motor impairment on the cylinder task, similarly to the comorbid Aβ/ET-1 model. Hindlimb motor function, which was tested in a beam-walk task, also appeared to be unaffected with no differences in the AHE scores noted between the groups (Fig. 3B). Rats who received an ischemic stroke had overall higher AHE scores (stroke effect $F_{(1,19)} = 4.858$, $p = 0.04$) suggesting a greater number of affected foot slips. There was no additional effect of comorbidity on the number of foot slips. However, APP21 TG comorbid rats showed an increase in total steps during the walk on day 21 vs baseline ($p = 0.026$; Fig. 3C), which suggested a potential change in their balance when being challenged to walk on a beam.

Cognitive function assessment: MWM

Comorbid $A\beta_{25-35}$ and ET-1 injected rats with intact spatial learning demonstrated long-term spatial reference memory impairment that was prevented with the antioxidant CAT-SKL treatment

All tested groups demonstrated good spatial learning as indicated by a significant decrease in latency and distance to reach the platform by the end of the training phase (day 8 vs day 11 $p < 0.0001$; Fig. 4A, B). All groups learned to the same extent as there was no difference between the groups on each day of learning. There was no significant difference in swim speed across all experimental groups on any of the testing days (Fig. 4C).

On day 12 post-surgery (Probe 1), 24 h following the last training day, all rats were comparable in the latency to the first entry to the TZ where the platform was located during the acquisition phase (Fig. 4D). Thus,

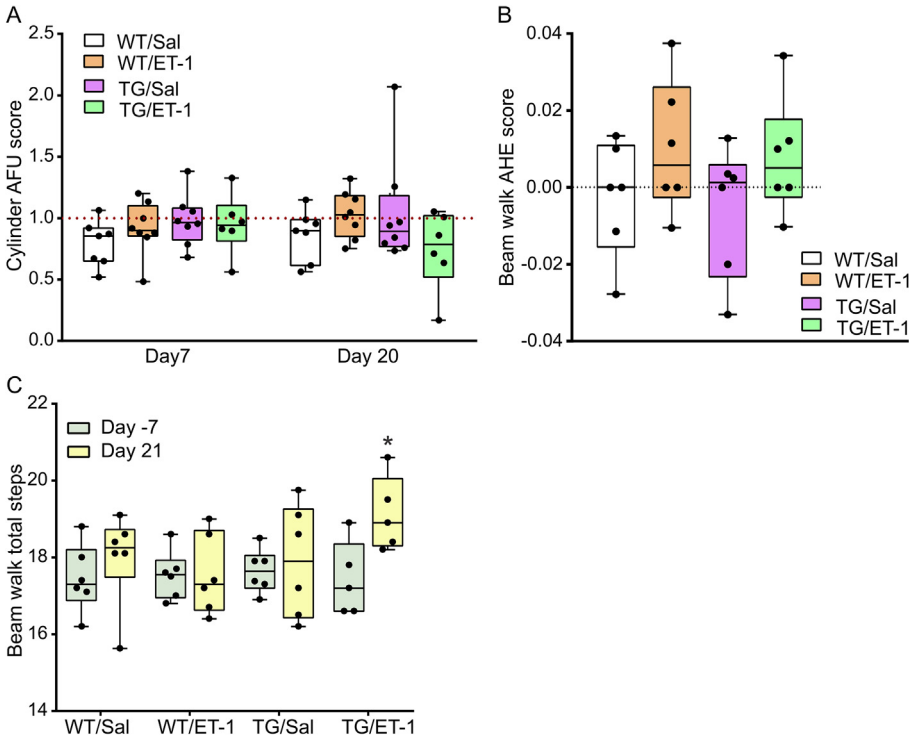

Fig. 3. Forelimb and hindlimb motor function of the comorbid APP21 TG Fischer 344 rat with ET-1 stroke model. **(A)** Affected (left) forelimb use (AFU) scores for the cylinder task. The red horizontal dotted line at y = 1.0 indicates an equal use of the forelimbs. A score of less than 1.0 represented a greater use of to the unaffected limb and a score of greater than 1.0 signified the opposite. Each bar represents values standardized to baseline and averaged for three trials per day. **(B)** Affected (left) hindlimb error scores (AHE score) for the beam walk task. Positive AHE score value represents a greater number of hindlimb errors made on post-surgery testing day. **(C)** Total number of steps on the beam-walk task. Data is presented as median (25th–75th percentiles). Repeated measurement two-way and one-way ANOVA, Tukey's post hoc test, $p < 0.05$. APP = amyloid precursor protein, ET-1 = endothelin-1, Sal = 0.9% saline, TG = APP21 transgenic Fischer 344 rat, WT = wildtype Fischer 344 rat. Significance is indicated by * in B) between beam-walk task days -7 and 21 for TG/ET-1 group ($p = 0.026$).

neither stroke or AD pathology alone, nor the comorbidity of two led to a short-term memory impairment in these rats.

On day 19 (Probe 2), one week following spatial learning, comorbid Aβ/ET-1 + Sal group was the only group who required significantly more time to enter the TZ compared to their Probe 1 ($p = 0.028$; Fig. 4D). This indicated a disturbance to the long-term memory of the platform location promoted by the co-presence of both stroke and increased cerebral amyloid burden. The swim speed measured for both probes was similar and therefore could not account for the detected differences (Fig. 4C). Thus, the observed effect was likely due to deficits in spatial memory retention and recall as a result of interaction between cerebral ischemia and amyloid toxicity. The treatment with CAT-SKL attenuated the memory deficits in the comorbid condition as no inter-probe difference was seen in the Aβ/ET-1 + CAT-SKL group (Fig. 4D).

Comorbid APP21 TG Fischer 344 rats with ET-1 ischemic stroke developed long-term spatial reference memory impairment while showing good spatial learning of the task

The comorbid TG/ET-1 rats were able to learn the platform location well in the spatial learning phase of the test since they had significantly decreased time and distance travelled until they found the platform by the last day of testing ($p < 0.0001$) and were comparable in their performance to all other groups (Fig. 5A, B). TG rats had overall a faster decrease in distance (genotype $F_{(1.29)} = 4.233 p = 0.0487$, time × genotype interaction $F_{(3.87)} = 3.320 p = 0.024$) and latency to platform (time × gene interaction $F_{(3.87)} = 3.475$ $p = 0.019$) with the task progression. Swim speed during all four testing days was not different between the groups (Fig. 5C).

The TG/ET-1 rats demonstrated a long-term reference memory deficit (Fig. 5D). The comorbid rats needed significantly more time to reach the TZ on Probe 2 compared to Probe 1 ($p = 0.03$, Fig. 5D). There was an inter-probe difference in swim speed noted for this group ($p = 0.001$, Fig. 5C). Therefore, to account for this fact, the latencies to the TZ entry were first standardized to a speed ratio on both probe days for each rat individually and then analyzed statistically. The latencies to first entry to the TZ as well as swim speed were similar between the experimental groups within each probe day (Fig. 5D).

Both $A\beta_{25–35}$–injected and APP21 TG Fischer 344 rat models comorbid with ET-1 ischemic stroke demonstrated good cued learning in the MWM

We did not observe any significant differences between the RP, $A\beta_{25–35}$ and ET-1 administered groups when analyzing latency and distance travelled to reach a platform with a figure mounted on top and above water level for this task (Fig. 6A, B). Swim speed was also not different (Fig. 6C).

Similarly, Fisher 344 rats showed comparable swim times and distances to cued platform and swim speed (Fig. 7). WT and TG rats with stroke overall showed longer latencies ($F_{(1.29)} = 7.046$ $p = 0.013$) and distances ($F_{(1.29)} = 8.789$ $p = 0.006$) to platform, however, swim speed was not different from non-stroke animals.

These results suggested that all groups in both models were equally motivated to find the escape platform and were able to use the cues for spatial navigation during MWM actual testing.

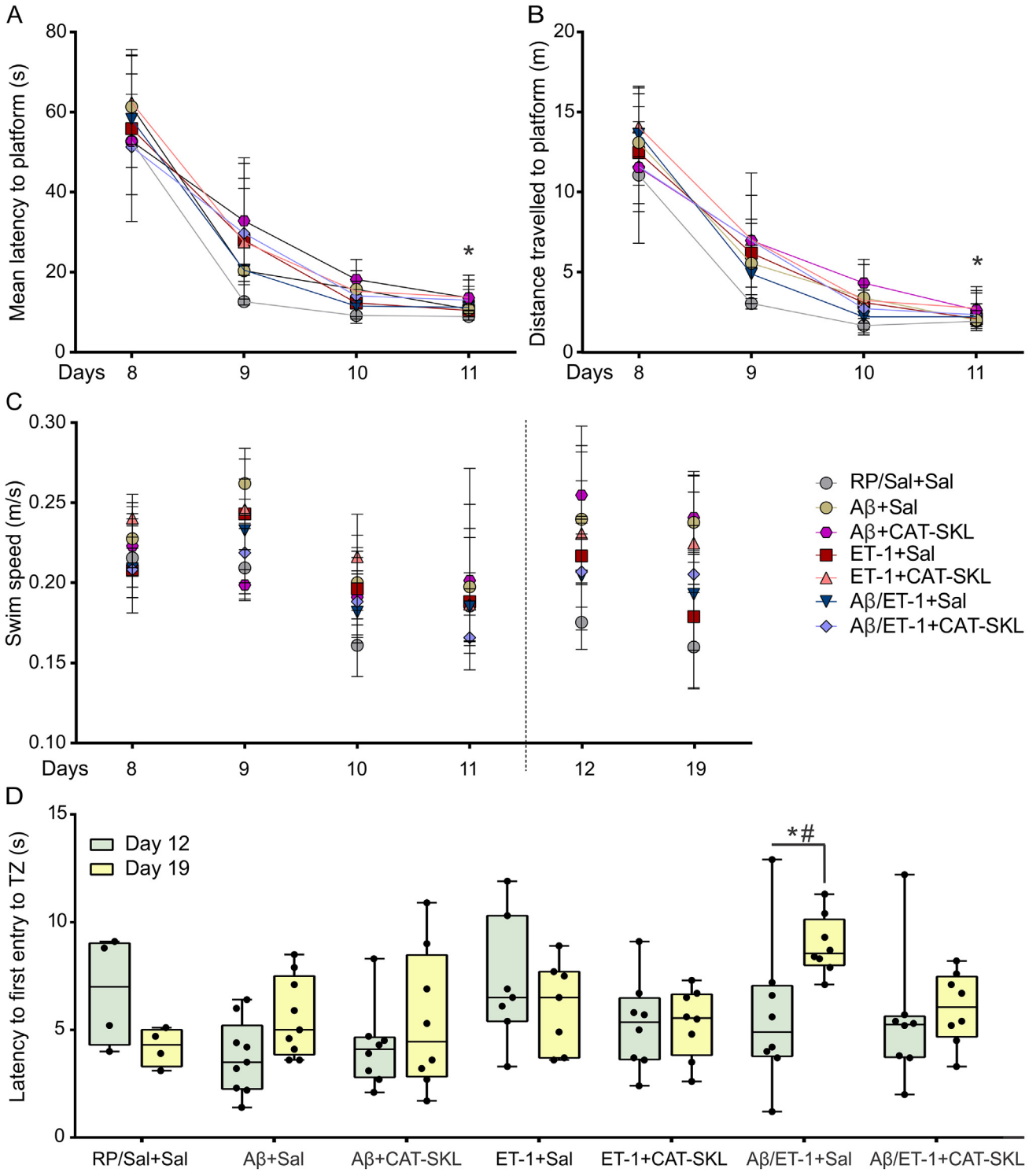

Fig. 4. Spatial learning and reference memory in the Morris water maze and the effect of the CAT-SKL treatment in the comorbid $A\beta_{25–35}$ – injected rats with ET-1 ischemic stroke. **(A)** Latency and **(B)** distance travelled to platform during spatial learning phase on days 8–11 post-surgery. **(C)** Swim speed for learning and probe days (days 12 and 19). **(D)** Latency to first entry to the target zone (TZ), which contained the hidden platform during the learning phase, in the probe trials on post-surgery days 12 and 19 as a measure of a short-term and long-term spatial reference memory, respectively. All values are presented as median (25th–75th percentiles). Repeated measurement two-way ANOVA, Tukey's and Bonferroni's (in **(C)**) post hoc tests, $p < 0.05$. Significance is represented with * for days 8 vs 11 in all groups in A, B ($p < 0.0001$) and for an inter-probe difference in Aβ/ET-1 + Sal group in **(D)** ($p = 0.028$); with # for Aβ/ET-1 + Sal vs RP/Sal + Sal ($p = 0.02$), vs ET-1 + CAT-SKL ($p = 0.037$) and vs Aβ + CAT-SKL ($p = 0.047$) within day 19. Aβ = amyloid $\beta_{25–35}$ peptide, CAT-SKL = genetically engineered cell penetrating variant of catalase with a serine-lysine-leucine carboxy terminal consensus sequence, ET-1 = endothelin-1, RP = reverse peptide ($A\beta_{35–25}$), Sal = 0.9% saline.

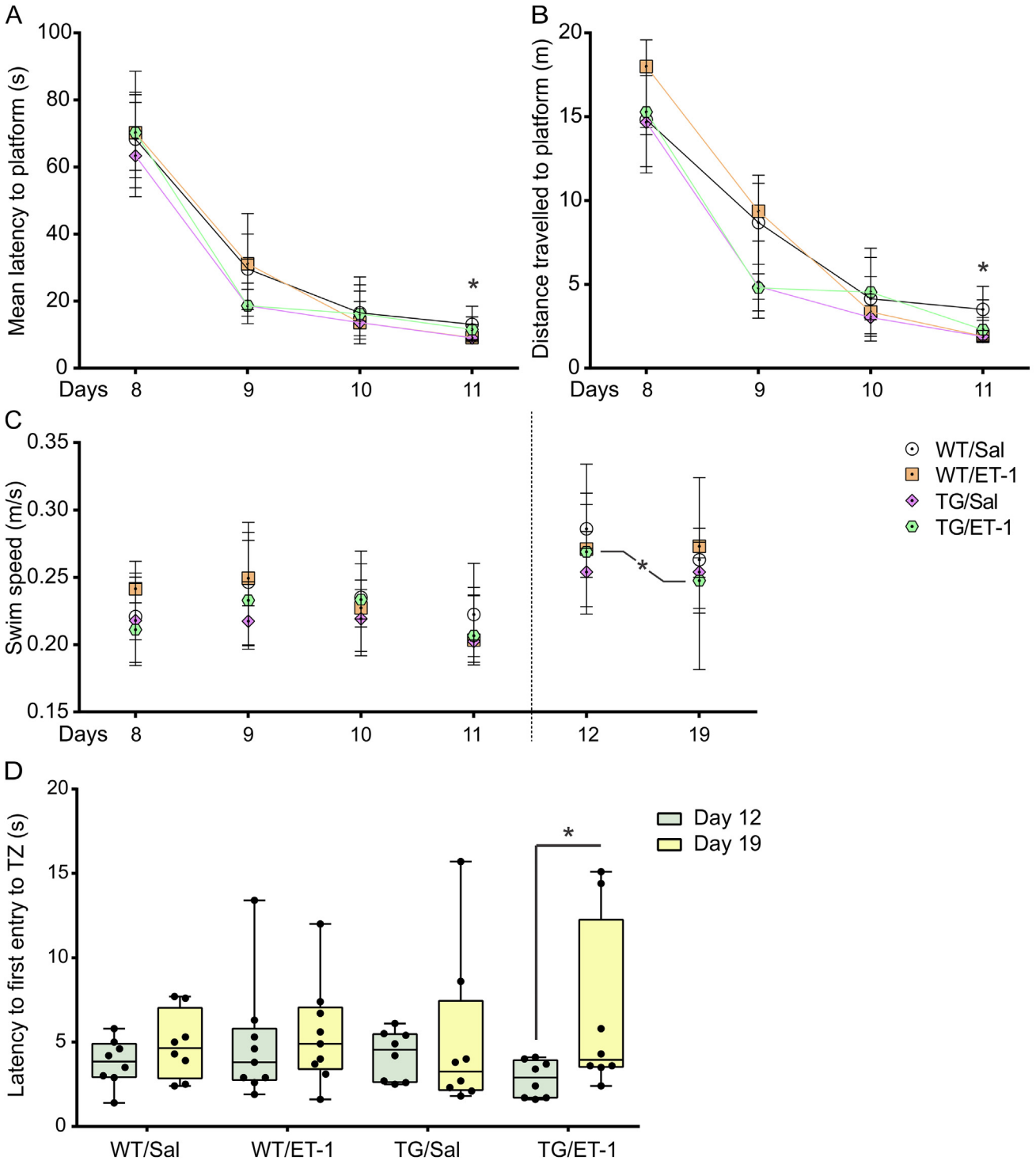

Fig. 5. Spatial reference memory in the Morris water maze of the comorbid APP21 TG Fischer 344 rat with ET-1 stroke model. **(A)** Latency and **(B)** distance travelled to platform during spatial learning phase on days 8–11 post-surgery. **(C)** Swim speed for learning and probe days (days 12 and 19). **(D)** Latency to first entry to the target zone (TZ), which contained the hidden platform during the learning phase, in the probe trials on post-surgery days 12 and 19 as a measure of spatial reference memory. Latencies presented as standardized to a speed ratio on both probe days. All values are presented as median (25th–75th percentiles). Repeated measurement two-way ANOVA, Bonferroni's post hoc tests, $p < 0.05$. Significance is represented with * for days 8 vs 11 in all groups in **(A)**, **(B)** ($p < 0.0001$); for an inter-probe difference in TG/ET-1 group in **(C)** ($p = 0.001$) and D ($p = 0.03$). APP = amyloid precursor protein, ET-1 = endothelin-1, Sal = 0.9% saline, TG = APP21 transgenic Fischer 344 rat, WT = wildtype Fischer 344 rat.

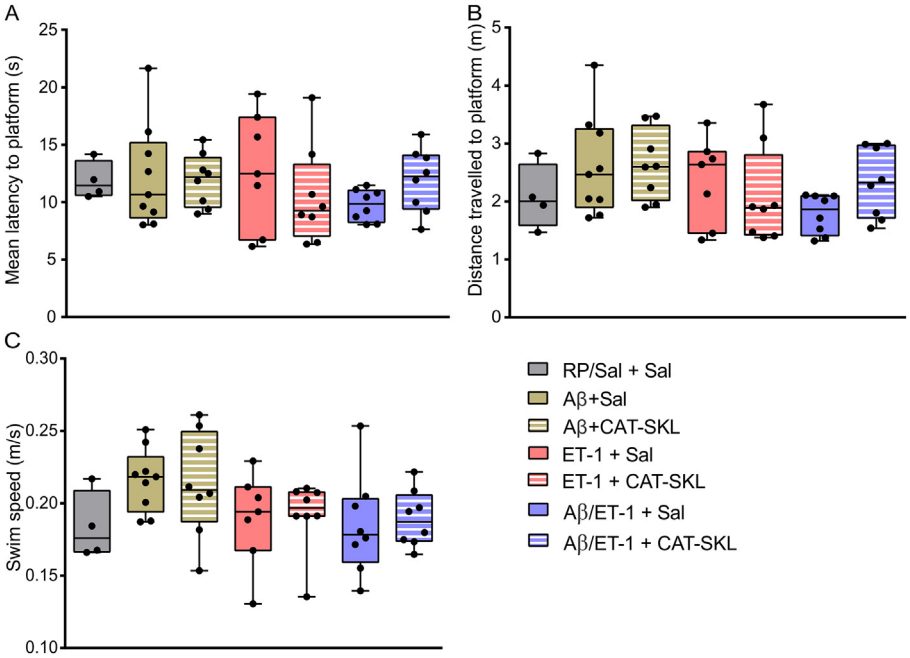

Fig. 6. Morris water maze cued learning of the comorbid $A\beta_{25–35}$ – injected rats with ET-1 ischemic stroke. **(A)** Latency and **(B)** distance to the hidden platform with a visible cue mounted on top. **(C)** Swim speed. Data presented as an average of all eight trials across two days of cued learning. Values are presented as the median (25th–75th percentiles). One-way ANOVA, Tukey's post hoc test, $p < 0.05$. Aβ = amyloid $\beta_{25–35}$ peptide, CAT-SKL = genetically engineered cell penetrating variant of catalase with a carboxy terminal serine-lysine-leucine peroxisomal targeting sequence, ET-1 = endothelin-1, RP = reverse peptide ($A\beta_{35–25}$), Sal = 0.9% saline.

Neuroinflammation: Microglia activation

We analyzed the effect of the comorbidity of ischemic stroke and AD-like pathology in its prodromal and early stages specifically on microglia activation within the cerebral infarct area, the striatum, and the basal forebrain (Figs. 8 and 9).

Comorbid $A\beta_{25–35}$–injected rats with ET-1 ischemic stroke developed increased microglial activation in the basal forebrain, but not in the striatum CAT-SKL antioxidant treatment ameliorating this pathology

There were no significant differences in the volume of OX-6 positive microglial inflammation in the right striatum across all groups (Fig. 8A, D). Thus, the comorbidity did not result in a greater inflammatory response at the ischemic lesion site at day 21 post-insult. However, the comorbid Aβ/ET-1 + Sal rats demonstrated a greater number of OX-6 immunoreactive microglia cells in the basal forebrain (co-presence of $A\beta_{25–35}$ with stroke effect; $F_{(1, 23)} = 9.043$, $p = 0.006$) compared to the stroke condition alone (vs. ET-1 + Sal $p = 0.01$, vs. ET-1 + CAT-SKL $p = 0.006$; Fig. 8B, C, E). This increase in microglia activation in the basal forebrain of the comorbid rats was attenuated by treatment with the antioxidant biologic CAT-SKL suggested by the cell counts in the Aβ/ET-1 + CAT-SKL rats, which were comparable to those in control and stroke alone groups (Fig. 8E).

Comorbid APP21 TG Fischer 344 rats with ET-1 ischemic stroke demonstrated increased microglial activation in the striatal infarct area, but not in the basal forebrain

Comorbid TG/ET-1 rats exhibited a significantly greater volume of OX-6 positive activated microglia in the striatal infarct region compared to their TG

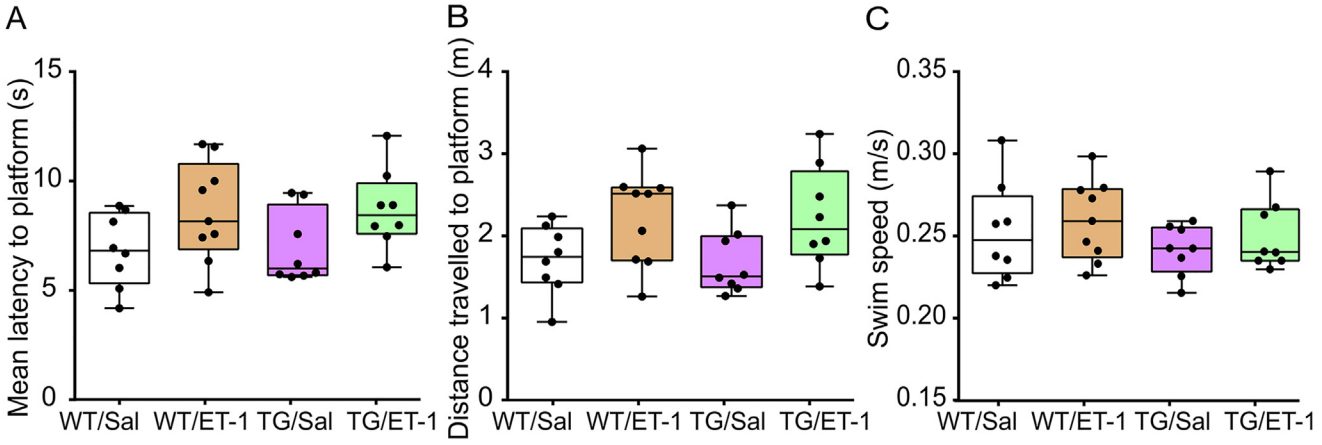

Fig. 7. Morris water maze cued learning of the comorbid APP21 TG Fischer 344 rat with ET-1 stroke model. **(A)** Latency and **(B)** distance to the hidden platform with a visible cue mounted on top. **(C)** Swim speed during cued trials. Data presented as an average of all eight trials across two days of cued learning. All values are presented as median (25th–75th percentiles). Repeated measurement two-way ANOVA, Bonferroni's post hoc tests, $p < 0.05$. APP = amyloid precursor protein, ET-1 = endothelin-1, Sal = 0.9% saline, TG = APP21 transgenic Fischer 344 rat, WT = wildtype Fischer 344 rat.

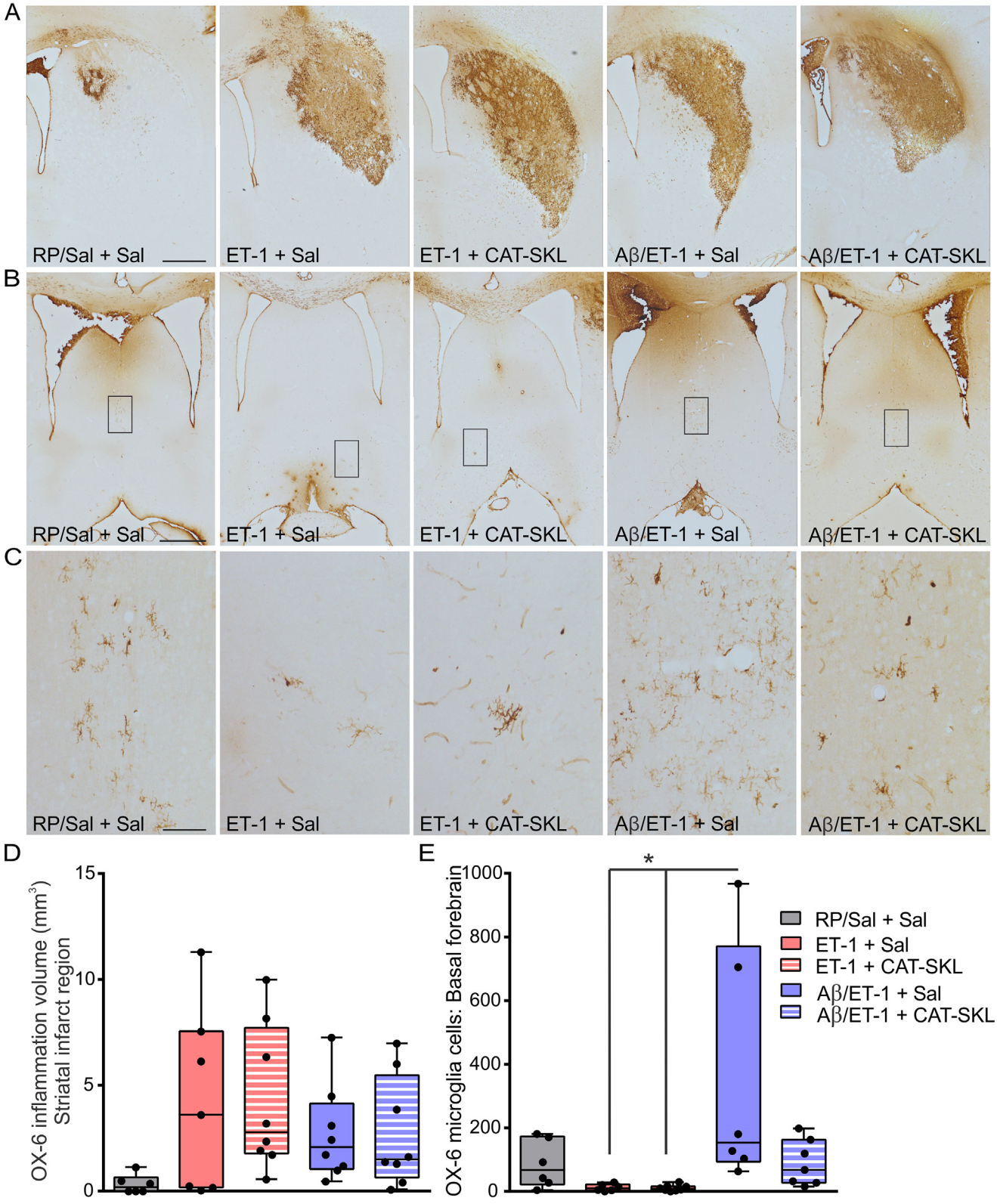

Fig. 8. Neuroinflammation in the comorbid $A\beta_{25-35}$ – injected rats with ET-1 ischemic stroke and effect of the CAT-SKL treatment. Representative 2× photomicrographs of OX-6 positive activated microglia within **(A)** the infarct region in the right striatum and **(B)** basal forebrain. **(C)** 10× images of activated microglia from corresponding boxed areas in **(B)**. Scale bar in **(A, B)** = 1 mm. Scale bar in **(C)** = 100 μm. **(D)** Volume of the right striatal inflammation based on the extent of OX-6 immunolabelled microglia. **(E)** Microglia cell count (cells/optical field) in the basal forebrain region. Animal numbers are as follows: RP/Sal + Sal $n = 6$, ET-1 + Sal $n = 7$ ($n = 6$ in **(E)**), ET-1 + CAT-SKL $n = 8$, Aβ/ET-1 + Sal $n = 8$ ($n = 6$ in **(E)**), Aβ/ET-1 + CAT-SKL $n = 8$ ($n = 7$ in **(E)**). Values are presented as the median (25th–75th percentiles) and significance is represented with * for Aβ/ET-1 + Sal rats vs. ET-1 + Sal ($p = 0.01$) and ET-1 + CAT-SKL ($p = 0.006$). One-way ANOVA, Tukey's post hoc test, $p < 0.05$. Aβ = amyloid β_{25-35} peptide, CAT-SKL = genetically engineered cell penetrating variant of catalase with a serine-lysine-leucine carboxy terminal consensus sequence, ET-1 = endothelin-1, RP = reverse peptide ($A\beta_{35-25}$), Sal = 0.9% saline.

counterparts (vs TG/Sal $p = 0.048$, Fig. 9A, D). While this same volume of inflammation was not significant compared to the control WT/Sal group, it was greater ($p = 0.0509$, Fig. 9D). The striatal inflammation volume in the stroke alone condition (WT/ET-1 rats) did not differ significantly from sham operated WT or TG rats (Fig. 9D). Thus, these results demonstrate a synergistic effect of a stroke within a pre-existing high APP and Aβ cerebral environment on microglia activation in the ischemic region.

There were no significant differences in the number of microglia present in the basal forebrain across surgical groups (Fig. 9B, C, E). The comorbid TG/ET-1 group tended to have greater levels of activated microglia compared to WT rats with or without stroke, but this effect was not significant ($p = 0.0515$ and $p = 0.0889$, Fig. 9E). TG rats overall had more OX-6 positive cells than WT rats (genotype effect $F_{(1.22)} = 7.034$ $p = 0.015$, Fig. 9E). This was in contrast to what was observed in the $A\beta_{25–35}$ infusion rat model of sporadic AD challenged with striatal stroke described above.

DISCUSSION

The results of this study demonstrate the detrimental impact of the comorbidity of prodromal (APP21 TG rat) and more degenerative ($A\beta_{25–35}$ ICV-injected rat) AD-like pathology with ET-1 ischemic stroke on spatial reference memory and microglia inflammation, specifically in the basal forebrain and striatal infarct zone. This work also shows for the first time a therapeutic potential of the antioxidant biologic CAT-SKL specifically in the comorbid AD and stroke condition.

ET-1 – induced ischemic stroke in the striatum, one of the brain regions involved in motor control, has previously been shown to produce motor impairment in rat models (Whitehead et al., 2005; Whitehead et al., 2005). In our study, stroke alone did not cause a gross impairment in the limb motor functioning in either model assessed using the cylinder and beam-walk tests. These tasks have been used to demonstrate motor dysfunction following a relatively large or multifocal stroke in other models (Clarke et al., 2007; Clarke et al., 2009; Lipsanen et al., 2011). It is possible that these tests were not sensitive enough to detect the possible motor changes caused by a smaller size striatal lesion which could occur at particular testing time points after stroke in our study. Although, an overall stroke effect on the hindlimb function was noted for the Fischer 344 rat model, no difference was observed when comparing performance between individual experimental groups. However, the comorbid TG rats of prodromal AD showed difficulties with balance suggested by the increase in total steps on the beam-walk. Interestingly, clinical studies have also previously indicated that alterations in gait and balance are present early in the disease process in AD patients, especially when cerebrovascular pathology is also present (Visser, 1983; Sheridan and Hausdorff, 2007; Inzitari et al., 2013). More specific tests such as the catwalk (Abada et al., 2013; Parkkinen et al., 2013) would be required to confirm the suggestion of potential gait disturbances resulting from the comorbidity of prodromal AD and stroke.

Somatosensory and especially fine motor deficits have been previously shown in animal models of stroke alone and with AD (Whitehead et al., 2005; Clarke et al., 2007; Cardoso et al., 2013). Analysis of our data from the MST task indicated only a transient sensorimotor deficit in the comorbid Aβ/ET-1 + Sal rats seen only on the first post-stroke testing day. It is possible that the size of ischemic lesion produced by striatal stroke in the $A\beta_{25–35}$ injection AD model was not large enough to cause a major disruption to somatosensory processes detectable at this stage of post-stroke recovery. The use of other specific tests including corner test and grid walking (Schaar et al., 2010) could aid in further elucidating the potential sensorimotor deficits following striatal stroke, which is important given the connection of the striatum to the somatosensory cortex.

Difficulties with spatial learning have been previously reported by other groups for rodent models of AD alone and when AD was paired with an extensive stroke (Choi et al., 2011; Zussy et al., 2011; Zussy et al., 2013). The analysis of the MWM task did not reveal any effect of the comorbidity on learning of the platform location in either model of AD in the present study. This could be attributed to a much smaller ischemic lesion limited to the striatum which could be insufficient to affect spatial learning or to earlier stages of AD recreated in our rats. Also, the time course of testing chosen here differs from aforementioned studies which detected the changes at later time points of several weeks post-stroke. An extended testing timeline could be implemented in future studies to characterize longer-term effects of the comorbid pathology.

There was a significant long-term spatial memory deficit observed in comorbid rats in both the APP21 TG and $A\beta_{25–35}$ – injected rat models. This was evidenced by an increase in the swim time to the TZ in search of a rescue platform, the position of which was learned earlier in the MWM. The absence of differences in swim speed, spatial and cued learning between animal groups described in the present manuscript and in (Au et al., 2016) allowed us to be confident that the observed memory impairment established in the comorbid condition was likely due to pathological events in the brain areas involved in spatial memory consolidation and recall. Neither stroke nor AD condition alone demonstrated this deficit, suggesting the potentiating effect of cerebral ischemia superimposed on a high brain amyloid environment via shared pathological processes.

Concurrent cerebral administration of $A\beta_{25–35}$ and striatal stroke resulted in a large increase in OX-6 positive activated microglial cells in the basal forebrain compared to the stroke only condition. The $A\beta_{25–35}$ – injected rat was previously reported to show significant OX-6 microgliosis in the basal forebrain which negatively correlated with cholinergic neuronal loss in that region and was suggested to be linked to spatial memory deficits observed in this rat model of AD (Nell et al., 2015; Nell et al., 2017). Our data further suggest microglial inflammation particularly in the basal forebrain

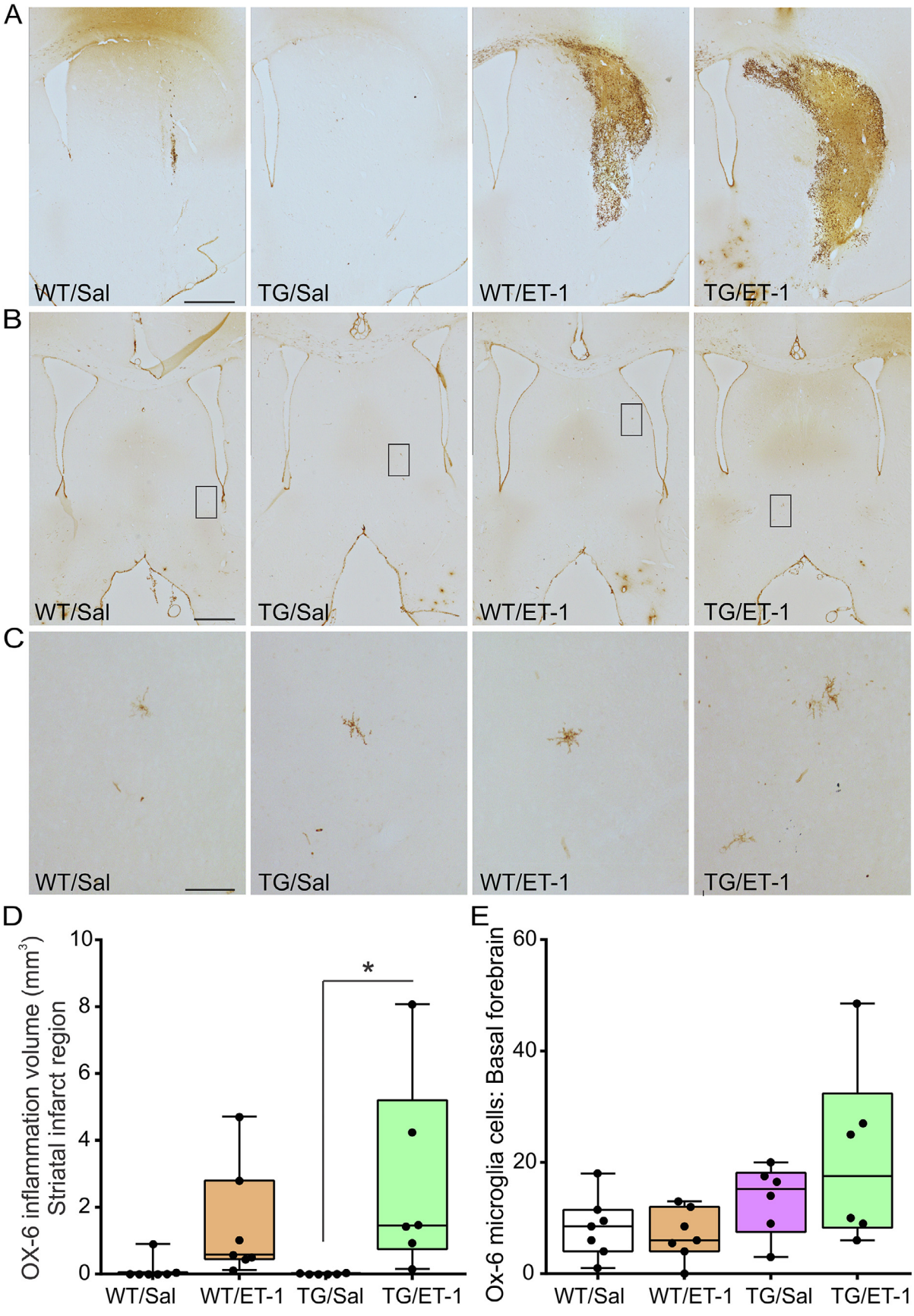
A
WT/Sal
TG/Sal
WT/ET-1
TG/ET-1
B
WT/Sal
TG/Sal
WT/ET-1
TG/ET-1
C
WT/Sal
TG/Sal
WT/ET-1
TG/ET-1
D
OX-6 inflammation volume (mm3)
Striatal infarct region
10
8
6
4
2
0
*
WT/Sal
WT/ET-1
TG/Sal
TG/ET-1
E
Ox-6 microglia cells: Basal forebrain
60
40
20
0
WT/Sal
WT/ET-1
TG/Sal
TG/ET-1

as a point of interaction between AD and stroke in the early disease stage which could lead to earlier establishment of cognitive symptoms in situations when both diseases are present in one individual compared to either condition alone. Along with the basal forebrain, a region highly vulnerable to AD, other brain areas implicated in the memory formation such as hippocampus were shown to be affected in AD. $A\beta_{25-35}$ – injected rats have been shown to develop increased gliosis and reduced neuronal number in the hippocampus (Whitehead et al., 2005; Nell et al., 2015). Comorbid $A\beta_{25-35}$/ET-1 rats in the present study could possibly develop an exacerbated hippocampal pathology, which could further contribute to the observed memory disturbances.

The volume of inflammation in the striatal infarct region of the stroke and $A\beta_{25-35}$ comorbid rats was unchanged from the level in the stroke alone rats. This was contrary to the results from earlier studies on three-month-old comorbid Wistar rats that showed a progressive increase in infarct size and associated regional inflammation compared to stroke alone rats who demonstrated a significant decrease in microglial inflammation in the infarct region by day 28 after stroke (Whitehead et al., 2005; Whitehead et al., 2007; Amtul et al., 2015). This discrepancy could be caused by the difference in the animal's age at the concurrent presentation of two insults. It has been shown that microglia cells transition to a chronically hyperactivatated state with increased age which contributes to formation of aberrant and persistent inflammatory reaction to an insult (Luo et al., 2010; Krstic and Knuesel, 2013; Perry and Holmes, 2014; Deleidi et al., 2015). It is possible that the six-month-old Wistar rats who received ET-1 stroke could have developed a more profound response to an ischemic lesion sustained by day 21 after stroke. These age-related events could blunt the difference in the OX-6 microglial response to stroke alone and to a sudden amyloid load introduced simultaneously. In addition to this, we used a higher concentration of ET-1 which could also have led to a bigger stroke and contributed to a maximized level of regional microgliosis.

On the contrary, the comorbid condition in the TG/ET1 rats resulted in increased levels of activated microglia in the infarct region compared to TG rats, but not WT/ET-1 rats (stroke alone). Aside from being a different strain, another principal difference between the APP21 TG model from the ICV $A\beta_{25-35}$ – injected rats is that there has already been increased cerebral APP and amyloid levels preceding the ischemic stroke in the APP21 TG rats. Developing amyloid pathology in conjunction with the events occurring during normal brain aging could increase brain vulnerability to ischemia and predispose the brain to a stronger response to stroke, such as the greater OX-6 microgliosis in the infarct region that was observed in our comorbid TG rats (Franceschi et al., 2007; Perry and Holmes, 2014). The striatal pathology could likely play a role in the motor and memory deficits seen in this group. This is in line with results of Whitehead et al., (Whitehead et al., 2007), who reported a cognitive impairment on the Barnes maze in the comorbid $A\beta_{25-35}$/ET-1 – injected rats, which had the greatest microgliosis in the striatal infarct zone.

APP21 TG Fischer 344 rats with stroke did not demonstrate an increase in activated microglia in the basal forebrain at least at day 21 post-stroke. It remains a question as to whether this phenomenon could be established at a later time point in the disease process. It is possible this model of prodromal AD might show a different pattern of microgliosis involving other brain areas more susceptible to ischemia in an environment with pre-existing chronically elevated APP and Aβ levels. In several studies, including those using the APP21 TG Fischer 344 rats, white matter has been shown to be particularly vulnerable in AD beginning in the prodromal stage and undergo pathological changes including increased microgliosis which were associated with cognitive impairment (Bilello, 2015; Brickman et al., 2015; Li et al., 2015; Raj et al., 2017; Weishaupt et al., 2018; Levit et al., 2019; Ivanova et al., 2020; Levit et al., 2020). It is possible that, aside from the increased inflammation in the immediate infarct zone, APP21 TG rats which sustained ischemic brain damage could develop increased inflammation in the white matter tracts and remote regions connected to the striatum, thus, contributing to memory disturbances observed in comorbid TG-ET-1 rats.

The present study focused specifically on microglial inflammation as one of the main and early pathologies in the disease in two highly vulnerable brain regions. However, AD is a multifactorial disease affecting multiple brain structures and alongside with inflammation and oxidative stress other events such synaptic dysfunction and white matter pathology are implicated in the disease pathogenesis. Therefore, further investigation is warranted to develop a comprehensive understanding of the brain changes in the event of comorbid cerebral ischemia in AD in both prodromal and early stages. It would also be of a great importance to characterize the interplay of stroke and AD in natural conditions occurring with increasing age in older age animals and at more advanced disease stages in the future studies. It is also necessary to carry

Fig. 9. Neuroinflammation: TG/ET-1 comorbid Fischer 344 rat model. Representative 2× photomicrographs of OX-6 positive activated microglia within **(A)** the right striatal infarct region and **(B)** basal forebrain. **(C)** 10× images of activated microglia presence in the basal forebrain from corresponding boxed areas in B. Scale bar in A and **(B)** = 1 mm. Scale bar in **(C)** = 100 μm. **(D)** Volume of the right striatal inflammation based on the extent of OX-6 immunolabelled microglia. **(E)** Microglia cell count (cells/optical field) in the basal forebrain region. Values are presented as the median (25th–75th percentiles) and significance is represented with * for TG/ET-1 rats vs TG/Sal ($p = 0.048$). Overall stroke effect in **(D)**: $F_{(1.22)} = 9.301$, $p = 0.006$. One-way, two-way ANOVA, Tukey's post hoc test, $p < 0.05$. ET-1 = endothelin-1, Sal = 0.9% saline, TG = transgenic (APP21 Fischer 344 rat), WT = wildtype (Fischer 344 rat).

out the experiments using female rats to elucidate the potential differences in effects of the comorbidity on behavioral and neuropathological aspects between biological sexes.

This work demonstrates the effectiveness of the targeted antioxidant CAT-SKL therapy against spatial memory impairment in a combined *in vivo* model of stroke and Aβ toxicity. The marked neuroprotective effect of the CAT-SKL was initially noticed *in vitro* (Giordano et al., 2015) and supported by earlier work of our group using a rat model of AD (Nell et al., 2017). In the current experiments we demonstrate the ability of the CAT-SKL treatment to attenuate increased activation of microglia in the basal forebrain as a result of AD comorbidity with stroke. This data further supports the role of interdependent oxidative stress and inflammation in mediating cognitive dysfunction in a comorbid AD and ischemic injury condition. The exact mechanism of CAT-SKL protection is a subject of a separate extensive exploration. One theory could be that the drug is acting through restoring cellular catalase levels, detoxifying hydrogen peroxide and subsequently decreasing ROS resulting from ischemia and AD pathology (Wood et al., 2006; Koepke et al., 2007; Undyala et al., 2011; Giordano and Terlecky, 2012; Giordano et al., 2015). Diminished oxidative stress reduces microglia activation and inflammatory damage to cholinergic neurons in the basal forebrain in particular and thus ameliorates cognitive deficit.

In the present study we have tested a single drug dose and administration route based on a previous successful protocol used *in vivo* (Nell et al., 2017). The treatment was initiated 1 week before injury, thus being a preventive measure and potentially increasing brain resilience to an insult. This could be applied to the clinical situations involving individuals with early stages of cognitive alterations such as mild neurocognitive disorder or early AD, who also have a high risk for developing a cerebrovascular accident, a common comorbidity in this age group and this patient cohort. It remains of great importance to establish the therapeutic potential of the CAT-SKL biologic in the case of administering it to a pre-existing high amyloid environment, such as in TG animals, or after induction of amyloid toxicity and stroke that would represent a more realistic clinical situation. Additionally, a detailed examination of a therapeutic window and minimum effective dose would also be required to complement the current study and advise on suitability of CAT-SKL use as a treatment.

In conclusion, this study suggests that microglia activation in the basal forebrain and infarct area in the striatum could be one of the pathologies mediating AD and ischemic stroke interaction and contributing to spatial memory and motor deficits in case of the comorbidity starting from the prodromal stage and continuing into a more advanced stage of AD development. The antioxidant biologic CAT-SKL showed a great therapeutic potential for prevention of exacerbation of inflammatory pathology and cognitive symptoms by the comorbidity of AD and stroke. This warrants further investigation into its use as a treatment strategy in individuals with coincidence of dementia and stroke.

ETHICAL APPROVAL

All animal handling and experimental procedures were approved by Western University Animal Care Committee (AUP 2008-113; AUP 2014-016) and were carried out in accordance with the guidelines of the Canadian Council on Animal Care and National Institute of Health Guide for the Care and Use of Laboratory Animals.

AVAILABILITY OF DATA AND MATERIALS

The datasets supporting the conclusions of this article are included within the article and its additional files.

FUNDING

This research was funded by an emerging team grant from the Canadian Institutes of Health Research (CIHR; R1478A47) to D. F. C. and CCNA team grant to S. N. W.

ACKNOWLEDGEMENTS

We are grateful to Lynn Wang (University of Western Ontario, London, Ontario, Canada) for her invaluable technical assistance. We thank Western University animal care facility for providing the animal care and Susanne Schmidt (University of Western Ontario, London, Ontario, Canada) for the use of behavioral equipment.

AUTHOR'S CONTRIBUTION

JLM completed acquisition, analysis, and interpretation of data. NI participated in data analysis, interpretation, and drafting of the manuscript. HJN acquired and provided cognitive testing data for a subset of animals. CA and YA developed the transgenic animal model. CRG participated in CAT-SKL purification and characterization. SRT and PAW developed, synthesized, purified and characterized the recombinant enzyme CAT-SKL. SNW participated in design of the work, data analysis and interpretation, and supervision of the work. DFC had primary role in design of the study, participated in the analysis and interpretation of the data and the writing of the manuscript and overall supervision of the work. All authors reviewed and approved the final manuscript.

CONFLICT OF INTERESTS

All authors declare no competing interests associated with this manuscript.

REFERENCES

Abada Y-se K, Nguyen HP, Schreiber R, Ellenbroek B, Nagai Y (2013) Assessment of motor function, sensory motor gating and recognition memory in a novel BACHD transgenic rat model for Huntington disease. PLoS ONE 8(7):e68584.

Agca C, Fritz JJ, Walker LC, Levey AI, Chan AWS, Lah JJ, Agca Y (2008) Development of transgenic rats producing human β-amyloid precursor protein as a model for Alzheimer's disease: Transgene and endogenous APP genes are regulated tissue-specifically. BMC Neurosci 9(1). https://doi.org/10.1186/1471-2202-9-28.

Akiyama H et al (2000) Inflammation and Alzheimer 's disease. Neurobiol Aging 21:383–421.

Allen CL, Bayraktutan U (2009) Oxidative stress and its role in the pathogenesis of ischaemic stroke. Int J Stroke 4(6):461–470.

Amtul Z (2015) Comorbid rat model of ischemia and β-Amyloid toxicity: Striatal and cortical degeneration. Brain Pathol 25 (1):24–32.

Amtul Z, Nikolova S, Gao L, Keeley RJ, Bechberger JF, Fisher AL, Bartha R, Munoz DG, McDonald RJ, Naus CC, Wojtowicz JM, Hachinski V, Cechetto DF (2014) Comorbid Aβ toxicity and stroke: hippocampal atrophy, pathology, and cognitive deficit. Neurobiol Aging 35(7):1605–1614.

Amtul Z, Whitehead SN, Keeley RJ, Bechberger J, Fisher AL, McDonald RJ, Naus CC, Munoz DG, Cechetto DF (2015) Comorbid rat model of ischemia and β-Amyloid toxicity: Striatal and cortical degeneration. Brain Pathol 25(1):24–32.

Attems J, Jellinger KA (2014) The overlap between vascular disease and Alzheimer's disease - lessons from pathology. BMC Med 12:206.

Au JL, Weishaupt N, Nell HJ, Whitehead SN, Cechetto DF (2016) Motor and hippocampal dependent spatial learning and reference memory assessment in a transgenic rat model of Alzheimer's disease with stroke. J Vis Exp 109.

Auld DS, Kornecook TJ, Bastianetto S, Quirion R (2002) Alzheimer's disease and the basal forebrain cholinergic system: relations to-amyloid peptides, cognition, and treatment strategies. Prog Neurobiol 68:209–245.

Bales KR, Du Y, Holtzman D, Cordell B, Paul SM (2000) Neuroinflammation and Alzheimer's disease: critical roles for cytokine/Abeta-induced glial activation, NF-kappaB, and apolipoprotein E. Neurobiol Aging 21:427–432.

Baudic S, Barba G, Thibaudet M, Smagghe A, Remy P, Traykov L (2006) Executive function deficits in early Alzheimer ' s disease and their relations with episodic memory. Arch Clin Neurophsychol 21(1):15–21.

Bilello M et al (2015) Correlating cognitive decline with white matter lesion and brain atrophy MRI measurements in Alzheimer's disease. J Alzheimers Dis 48:987–994.

Brickman AM, Zahodne LB, Guzman VA, Narkhede A, Meier IB, Griffith EY, Provenzano FA, Schupf N, Manly JJ, Stern Y, Luchsinger JA, Mayeux R (2015) Reconsidering harbingers of dementia: Progression of parietal lobe white matter hyperintensities predicts Alzheimer's disease incidence. Neurobiol Aging 36(1):27–32.

Cardoso MM, Franco ECS, de Souza CC, da Silva MC, Gouveia A, Gomes-Leal W (2013) Minocycline treatment and bone marrow mononuclear cell transplantation after endothelin-1 induced striatal ischemia. Inflammation 36(1):197–205.

Caughlin S, Maheshwari S, Agca Y, Agca C, Harris AJ, Jurcic K, Yeung K-C, Cechetto DF, Whitehead SN (2018) Membrane-lipid homeostasis in a prodromal rat model of Alzheimer's disease: Characteristic profiles in ganglioside distributions during aging detected using MALDI imaging mass spectrometry. Biochim Biophys Acta - Gen Subj 1862(6):1327–1338.

Cechetto DF, Hachinski V, Whitehead SN (2008) Vascular risk factors and Alzheimer 's disease. Expert Rev Neurother 8 (5):743–750.

Cheng G, Whitehead SN, Hachinski V, Cechetto DF (2006) Effects of pyrrolidine dithiocarbamate on beta-amyloid (25–35)-induced inflammatory responses and memory deficits in the rat. Neurobiol Dis 23(1):140–151.

Choi B-R, Lee SR, Han J-S, Woo S-K, Kim KM, Choi D-H, Kwon KJ, Han S-H, Shin CY, Lee J, Chung C-S, Lee S-R, Kim HY (2011) Synergistic memory impairment through the interaction of chronic cerebral hypoperfusion and amlyloid toxicity in a rat model. Stroke 42(9):2595–2604.

Clarke J, Thornell A, Corbett D, Soininen H, Hiltunen M, Jolkkonen J (2007) Overexpression of APP provides neuroprotection in the absence of functional benefit following middle cerebral artery occlusion in rats. Eur J Neurosci 26(7):1845–1852.

Clarke J, Mala H, Windle V, Chernenko G, Corbett D (2009) The effects of repeated rehabilitation tune-ups on functional recovery after focal ischemia in rats. Neurorehab Neural Repair 23 (9):886–894.

Collerton D (1989) Cholinergic function and intellectual decline in. Neuroscience 19:1–28.

Combs CK, Karlo JC, Kao S-C, Landreth GE (2001) Amyloid stimulation of microglia and monocytes results in TNF-dependent expression of inducible nitric oxide synthase and neuronal apoptosis. J Neurosci 21:1179–1188.

Craig LA, Hong NS, McDonald RJ (2011) Revisiting the cholinergic hypothesis in the development of Alzheimer's disease. Neurosci Biobehav Rev 35(6):1397–1409.

Del Ser T, Hachinski V, Merskey H, Munoz DG (2005) Alzheimer's disease with and without cerebral infarcts. J Neurol Sci 231(1-2):3–11.

Deleidi M, Jäggle M, Rubino G (2015) Immune ageing, dysmetabolism and inflammation in neurological diseases. Front Neurosci 9:1–14.

Esiri MM, Nagy Z, Smith MZ, Barnetson L, Smith AD (1999) Cerebrovascular disease and threshold for dementia in the early stages of Alzheimer's disease. Lancet 354(9182):919–920.

Fischer R, Maier O (2015) Interrelation of oxidative stress and inflammation in neurodegenerative disease: role of TNF. Oxid Med Cell Longevity 2015:1–18.

Franceschi C, Capri M, Monti D, Giunta S, Olivieri F, Sevini F, Panourgia MP, Invidia L, Celani L, Scurti M, Cevenini E, Castellani GC, Salvioli S (2007) Inflammaging and anti-inflammaging: A systemic perspective on aging and longevity emerged from studies in humans. Mech Ageing Dev 128 (1):92–105.

Geula C, Nagykery N, Nicholas A, Wu C-K (2008) Cholinergic neuronal and axonal abnormalities are present early in aging and in Alzheimer disease. J Neuropathol Exp Neurol 67(4):309–318.

Giordano CR, Terlecky SR (2012) Peroxisomes, cell senescence, and rates of aging. Biochim Biophys Acta 1822(9):1358–1362.

Giordano CR, Terlecky LJ, Bollig-Fischer A, Walton PA, Terlecky SR (2015) Amyloid-beta neuroprotection mediated by a targeted antioxidant. Sci Rep 4(1).

Grober ELLEN, Hall CB, Lipton RB, Zonderman AB, Resnick SM, Kawas CLAUDIA (2008) Memory impairment, executive dysfunction, and intellectual decline in preclinical Alzheimer ' s disease. J Int Neuropsychol Soc 14(2):266–278.

Heneka MT, Carson MJ, Khoury JE, Landreth GE, Brosseron F, Feinstein DL, Jacobs AH, Wyss-Coray T, Vitorica J, Ransohoff RM, Herrup K, Frautschy SA, Finsen B, Brown GC, Verkhratsky A, Yamanaka K, Koistinaho J, Latz E, Halle A, Petzold GC, Town T, Morgan D, Shinohara ML, Perry VH, Holmes C, Bazan NG, Brooks DJ, Hunot S, Joseph B, Deigendesch N, Garaschuk O, Boddeke E, Dinarello CA, Breitner JC, Cole GM, Golenbock DT, Kummer MP (2015) Neuroinflammation in Alzheimer's disease. Lancet Neurol 14(4):388–405.

Heyman A, Fillenbaum GG, Welsh-Bohmer KA, Gearing M, Mirra SS, Mohs RC, Peterson BL, Pieper CF (1998) Cerebral infarcts in patients with autopsy-proven Alzheimer's disease CERAD, part XVIII. Neurology 51(1):159–162.

Inzitari M, Gine-Garriga M, Martinez B, Perez-Fernandez M, Barranco-Rubia E, Lleo A, Salva-Casanovas A (2013) Cerebrovascular disease and gait and balance impairment in mild to moderate Alzheimer's disease. J Nutr Health Aging 17 (1):45–48.

Ivanova N, Liu Q, Agca C, Agca Y, Noble EG, Whitehead SN, Cechetto DF (2020) White matter inflammation and cognitive function in a co-morbid metabolic syndrome and prodromal

Alzheimer's disease rat model. J Neuroinflamm 17(1). https://doi.org/10.1186/s12974-020-1698-7.
Kadowaki H, Nishitoh H, Urano F, Sadamitsu C, Matsuzawa A, Takeda K, Masutani H, Yodoi J, Urano Y, Nagano T, Ichijo H (2005) Amyloid β induces neuronal cell death through ROS-mediated ASK1 activation. Cell Death Differ 12(1):19–24.
Kalaria RN (2000) The role of cerebral ischemia in Alzheimer's disease. Neurobiol Aging 21(2):321–330.
Kinney JW, Bemiller SM, Murtishaw AS, Leisgang AM, Salazar AM, Lamb BT (2018) Inflammation as a central mechanism in Alzheimer's disease. Alzheimers Dementia Transl Res Clin Interv 4(1):575–590.
Klakotskaia D, Agca C, Richardson RA, Stopa EG, Schachtman TR, Agca Y, Ginsberg SD (2018) Memory deficiency, cerebral amyloid angiopathy, and amyloid-β plaques in APP + PS1 double transgenic rat model of Alzheimer's disease. PLoS ONE 13(4): e0195469.
Koepke JI, Nakrieko K-A, Wood CS, Boucher KK, Terlecky LJ, Walton PA, Terlecky SR (2007) Restoration of peroxisomal catalase import in a model of human cellular aging. Traffic 8 (11):1590–1600.
Kowall NW, McKee AC, Yankner BA, Beal MF (1992) In vivo neurotoxicity of beta-amyloid [β(1–40)] and the β(25–35) fragment. Neurobiol Aging 13(5):537–542.
Krstic D, Knuesel I (2013) Deciphering the mechanism underlying late-onset Alzheimer disease. Nat Rev Neurol 9(1):25–34.
Kubo T, Nishimura S, Kumagae Y, Kaneko I (2002) In vivo conversion of racemized βamyloid ([D-Ser26]Aβ1-40) to truncated and toxic fragments ([D-Ser26]Aβ25-35/40) and fragment presence in the brains of Alzheimer's patients. J Neurosci Res 70:474–483.
Lakhan SE, Kirchgessner A, Hofer M (2009) Inflammatory mechanisms in ischemic stroke: Therapeutic approaches. J Transl Med 7(1).
Lee S, Viqar F, Zimmerman ME, Narkhede A, Tosto G, Benzinger TLS, Marcus DS, Fagan AM, Goate A, Fox NC, Cairns NJ, Holtzman DM, Buckles V, Ghetti B, McDade E, Martins RN, Saykin AJ, Masters CL, Ringman JM, Ryan NS, Förster S, Laske C, Schofield PR, Sperling RA, Salloway S, Correia S, Jack C, Weiner M, Bateman RJ, Morris JC, Mayeux R, Brickman AM (2016) White matter hyperintensities are a core feature of Alzheimer's disease: Evidence from the Dominantly Inherited Alzheimer Network. Annu Neurol 79(6):929–939.
Levit A, Regis AM, Garabon JR, Oh S-H, Desai SJ, Rajakumar N, Hachinski V, Agca Y, Agca C, Whitehead SN, Allman BL (2017) Behavioural inflexibility in a comorbid rat model of striatal ischemic injury and mutant hAPP overexpression. Behav Brain Res 333:267–275.
Levit A, Regis AM, Gibson A, Hough OH, Maheshwari S, Agca Y, Agca C, Hachinski V, Allman BL, Whitehead SN (2019) Impaired behavioural flexibility related to white matter microgliosis in the TgAPP21 rat model of Alzheimer disease. Brain Behav Immun 80:25–34.
Levit A, Cheng S, Hough O, Liu Q, Agca Y, Agca C, Hachinski V, Whitehead SN (2020) Hypertension and pathogenic hAPP independently induce white matter astrocytosis and cognitive impairment in the rat. Front Aging Neurosci 12.
Li X, Westman E, Ståhlbom AK, Thordardottir S, Almkvist O, Blennow K, Wahlund L-O, Graff C (2015) White matter changes in familial Alzheimer's disease. J Intern Med 278(2):211–218.
Lipsanen A, Hiltunen M, Jolkkonen J (2011) Chronic ibuprofen treatment does not affect the secondary pathology in the thalamus or improve behavioral outcome in middle cerebral artery occlusion rats. Pharmacol Biochem Behav 99(3):468–474.
Luo X-G, Ding J-Q, Chen S-D (2010) Microglia in the aging brain: relevance to neurodegeneration. Mol Neurodegener 5:12.
Madigan JB, Wilcock DM, Hainsworth AH (2016) Vascular contributions to cognitive impairment and dementia: Topical review of animal models. Stroke 47(7):1953–1959.
McGeer EG, McGeer PL (2003) Inflammatory processes in Alzheimer's disease. Prog Neuro-Psychopharmacol Biol Psychiatry 27(5):741–749.
Millucci L, Raggiaschi R, Franceschini D, Terstappen G, Santucci A (2009) Rapid aggregation and assembly in aqueous solution of Aβ (25–35) peptide. J Biosci 34(2):293–303.
Nell HJ, Whitehead SN, Cechetto DF (2015) Age-dependent effect of β-amyloid toxicity on basal forebrain cholinergic neurons and inflammation in the rat brain. Brain Pathol 25(5):531–542.
Nell HJ, Au JL, Giordano CR, Terlecky SR, Walton PA, Whitehead SN, Cechetto DF (2017) Targeted antioxidant, catalase-SKL, reduces beta-amyloid toxicity in the rat brain. Brain Pathol 27 (1):86–94.
Nogawa S, Zhang F, Ross ME, Iadecola C (1997) Cyclo-oxygenase-2 gene expression in neurons contributes to ischemic brain damage. J Neurosci 17(8):2746–2755.
Nunomura A, Perry G, Aliev G, Hirai K, Takeda A, Balraj EK, Jones PK, Ghanbari H, Wataya T, Shimohama S, Chiba S, Atwood CS, Petersen RB, Smith MA (2001) Oxidative damage is the earliest event in Alzheimer disease. J Neuropathol Exp Neurol 60 (8):759–767.
Parkkinen S, Ortega FJ, Kuptsova K, Huttunen J, Tarkka I, Jolkkonen J (2013) Gait impairment in a rat model of focal cerebral ischemia. Stroke Res Treat 2013:1–12. https://doi.org/10.1155/2013/410972.
Paxinos G, Watson C (1986) The rat brain in stereotaxic coordinates. Academic Press Inc.
Perry VH, Holmes C (2014) Microglial priming in neurodegenerative disease. Nature Rev Neurol 10(4):217–224.
Pike CJ, Walencewicz-Wasserman AJ, Kosmoski J, Cribbs DH, Glabe CG, Cotman CW (1995) Structure-activity analyses of β-amyloid peptides: contributions of the β25-35 region to aggregation and neurotoxicity. J Neurochem 64(1):253–265.
Prins ND, Scheltens P (2015) White matter hyperintensities, cognitive impairment and dementia: an update. Nature Rev Neurol 11:157–165.
Public Health Agency of Canada. (2020). Dementia and stroke comorbidity among Canadians aged 65 years and older: highlights from the Canadian chronic disease surveillance system.
Raj D, Yin Z, Breur M, Doorduin J, Holtman IR, Olah M, Mantingh-Otter IJ, Van Dam D, De Deyn PP, den Dunnen W, Eggen BJL, Amor S, Boddeke E (2017) Increased white matter inflammation in aging- and Alzheimer's disease brain. Front Mol Neurosci 10. https://doi.org/10.3389/fnmol.2017.00206.
Regan C, Katona C, Walker Z, Hooper J, Donovan J, Livingston G (2006) Relationship of vascular risk to the progression of Alzheimer disease. Neurology 67(8):1357–1362.
Rosen RF et al (2012) Exogenous seeding of cerebral β-amyloid in βAPP -transgenic rats. J Neurochem 120:660–666.
Schaar KL, Brenneman MM, Savitz SI (2010) Functional assessments in the rodent stroke model. Exp Transl Stroke Med 2(1). https://doi.org/10.1186/2040-7378-2-13.
Schallert T, Woodlee MT, Fleming SM (2002) Disentangling multiple types of recovery from brain injury. Pharmacol Cereb Ischemia:201–216.
Schliebs R (2005) Basal forebrain cholinergic dysfunction in Alzheimer's disease - Interrelationship with β-amyloid, inflammation and neurotrophin signaling. Neurochem Res 30(6-7):895–908.
Schneider JA, Boyle PA, Arvanitakis Z, Bienias JL, Bennett DA (2007) Subcortical infarcts, Alzheimer's disease pathology, and memory function in older persons. Ann Neurol 62(1):59–66.
Sheridan PL, Hausdorff JM (2007) The role of higher-level cognitive function in gait: Executive dysfunction contributes to fall risk in Alzheimer's disease. Dement Geriatr Cogn Disord 24 (2):125–137.
Sigurdsson EM, Lee JM, Dong X-W, Hejna MJ, Lorens SA (1997) Bilateral injections of amyloid-β 25–35 into the amygdala of young

Fischer rats: Behavioral, neurochemical, and time dependent histopathological effects. Neurobiol Aging 18(6):591–608.
Silverberg GD, Miller MC, Pascale CL, Caralopoulos IN, Agca Y, Agca C, Stopa EG (2015) Kaolin-induced chronic hydrocephalus accelerates amyloid deposition and vascular disease in transgenic rats expressing high levels of human APP. Fluids Barriers CNS 12(1). https://doi.org/10.1186/2045-8118-12-2.
Snowdon DA (1997) Aging and Alzheimer's disease: lessons from the Nun Study. The Gerontologist 37(2):150–156.
Snowdon DA et al (1997) Brain infarction and the clinical expression of Alzheimer disease: The Nun Study. JAMA J Am Med Assoc 277:813–817.
Stoll G, Jander S, Schroeter M (1998) Inflammation and glial responses in ischemic brain lesions. Prog Neurobiol 56:149–171.
Sughrue ME, Mocco J, Komotar RJ, Mehra A, D'Ambrosio AL, Grobelny BT, Penn DL, Connolly ES (2006) An improved test of neurological dysfunction following transient focal cerebral ischemia in rats. J Neurosci Methods 151(2):83–89.
Tatemichi TK et al. (1992) Dementia after stroke: Baseline frequency, risks, and clinical features in a hospitalized cohort. Neurology 42:1185–1193.
Taylor CA, Bouldin ED, Greenlund KJ, Mcguire LC. (2020) Comorbid chronic conditions among older adults with subjective cognitive decline, United States, 2015-2017. Innovat Aging 4.
Thiel A, Radlinska BA, Paquette C, Sidel M, Soucy J-P, Schirrmacher R, Minuk J (2010) The temporal dynamics of poststroke neuroinflammation: A longitudinal diffusion tensor imaging-guided PET study with 11C-PK11195 in acute subcortical stroke. J Nucl Med 51(9):1404–1412.
Thiel A, Cechetto DF, Heiss W-D, Hachinski V, Whitehead SN (2014) Amyloid burden, neuroinflammation, and links to cognitive decline after ischemic stroke. Stroke 45(9):2825–2829.
Toledo JB, et al. (2013) Contribution of cerebrovascular disease in autopsy confirmed neurodegenerative disease cases in the National Alzheimer's Coordinating Centre. Brain 136; 2697–2706.
Undyala V, Terlecky SR, Vander Heide RS (2011) Targeted intracellular catalase delivery protects neonatal rat myocytes from hypoxia-reoxygenation and ischemia-reperfusion injury. Cardiovasc Pathol 20(5):272–280.
Venkateshappa C, Harish G, Mahadevan A, Srinivas Bharath MM, Shankar SK (2012) Elevated oxidative stress and decreased antioxidant function in the human hippocampus and frontal cortex with increasing age. Neurochem Res 37(8):1601–1614.
Vermeer SE, Prins ND, den Heijer T, Hofman A, Koudstaal PJ, Breteler MMB (2003) Silent brain infarcts and the risk of dementia and cognitive decline. N Engl J Med 348(13):1215–1222.
Visser H (1983) Gait and balance in senile dementia of Alzheimer's type. Age Ageing 12(4):296–301.
Vorhees CV, Williams MT (2006) Morris water maze: procedures for assessing spatial and related forms of learning and memory. Nat Protocols 1(2):848–858.
Vorhees CV, Williams MT (2014) Assessing spatial learning and memory in rodents. ILAR J 55(2):310–332.
Weinstein JR, Koerner IP, Möller T (2010) Microglia in ischemic brain injury. Future Neurol 5(2):227–246.
Weishaupt N, Liu Q, Shin S, Singh R, Agca Y, Agca C, Hachinski V, Whitehead SN (2018) APP21 transgenic rats develop age-dependent cognitive impairment and microglia accumulation within white matter tracts. J Neuroinflamm 15(1). https://doi.org/10.1186/s12974-018-1273-7.
Whitehead S, Cheng G, Hachinski V, Cechetto DF (2005) Interaction between a rat model of cerebral ischemia and β-amyloid toxicity: II. Effects of triflusal. Stroke 36(8):1782–1789.
Whitehead SN, Hachinski VC, Cechetto DF (2005) Interaction between a rat model of cerebral ischemia and β-amyloid toxicity: Inflammatory responses. Stroke 36(1):107–112.
Whitehead SN, Cheng G, Hachinski VC, Cechetto DF (2007) Progressive increase in infarct size, neuroinflammation, and cognitive deficits in the presence of high levels of amyloid. Stroke 38(12):3245–3250.
Whitehead SN, Massoni E, Cheng G, Hachinski VC, Cimino M, Balduini W, Cechetto DF (2010) Triflusal reduces cerebral ischemia induced inflammation in a combined mouse model of Alzheimer's disease and stroke. Brain Res 1366:246–256.
Whitehouse PJ, Price DL, Struble RG, Clark AW, Coyle JT, DeLong MR (1982) Alzheimer's disease and senile dementia: loss of neurons in the basal forebrain. Science 215(4537):1237–1239.
Wojsiat J, Zoltowska KM, Laskowska-Kaszub K, Wojda U (2018) Oxidant/antioxidant imbalance in Alzheimer's disease: therapeutic and diagnostic prospects. Oxid Med Cell Longevity 2018:1–16.
Wood CS, Koepke JI, Teng H, Boucher KK, Katz S, Chang P, Terlecky LJ, Papanayotou I, Walton PA, Terlecky SR (2006) Hypocatalasemic fibroblasts accumulate hydrogen peroxide and display age-associated pathologies. Traffic 7(1):97–107.
Wyss-Coray T (2006) Inflammation in Alzheimer disease: driving force, bystander or beneficial response? Nat Med 12:1005–1015.
Yanagisawa M, Kurihara H, Kimura S, Tomobe Y, Kobayashi M, Mitsui Y, Yazaki Y, Goto K, Masaki T (1988) A novel potent vasoconstrictor peptide produced by vascular endothelial cells. Nature 332(6163):411–415.
Yang J, D'Esterre CD, Amtul Z, Cechetto DF, Lee TY (2014) Hemodynamic effects of combined focal cerebral ischemia and amyloid protein toxicity in a rat model: A functional CT study. PLoS ONE 9:1–8.
Yankner BA, Dawes LR, Fisher S, Villa-Komaroff L, Oster-Granite ML, Neve RL (1989) Neurotoxicity of a fragment of the amyloid precursor associated with Alzheimer's Disease. Science 245 (4916):417–420.
Young CN, Koepke JI, Terlecky LJ, Borkin MS, Boyd SL, Terlecky SR (2008) Reactive oxygen species in tumor necrosis factor-α-activated primary human keratinocytes: Implications for psoriasis and inflammatory skin disease. J Invest Dermatol 128 (11):2606–2614.
Zhou J, Yu J-T, Wang H-F, Meng X-F, Tan C-C, Wang J, Wang C, Tan L (2014) Association between stroke and Alzheimer's disease: Systematic review and meta-analysis. J Alzheimers Dis 43(2):479–489.
Zussy C, Brureau A, Delair B, Marchal S, Keller E, Ixart G, Naert G, Meunier J, Chevallier N, Maurice T, Givalois L (2011) Time-course and regional analyses of the physiopathological changes induced after cerebral injection of an amyloid β fragment in rats. Am J Pathol 179(1):315–334.
Zussy C, Brureau A, Keller E, Marchal S, Blayo C, Delair B, Ixart G, Maurice T, Givalois L, Ginsberg SD (2013) Alzheimer's disease related markers, cellular toxicity and behavioral deficits induced six weeks after oligomeric amyloid-β peptide injection in rats. PLoS ONE 8(1):e53117.

(Received 2 November 2021, Accepted 28 January 2022)
(Available online 03 February 2022)